

On geodesic triangles with right angles in a dually flat space*

Frank Nielsen[†]

Sony Computer Science Laboratories, Inc.
Tokyo, Japan

Abstract

The dualistic structure of statistical manifolds in information geometry yields eight types of geodesic triangles passing through three given points, the triangle vertices. The interior angles of geodesic triangles can sum up to π like in Euclidean/Mahalanobis flat geometry, or exhibit otherwise angle excesses or angle defects. In this paper, we initiate the study of geodesic triangles in dually flat spaces, termed Bregman manifolds, where a generalized Pythagorean theorem holds. We consider non-self dual Bregman manifolds since Mahalanobis self-dual manifolds amount to Euclidean geometry. First, we show how to construct geodesic triangles with either one, two, or three interior right angles, whenever it is possible. Second, we report a construction of triples of points for which the dual Pythagorean theorems hold simultaneously at a point, yielding two dual pairs of dual-type geodesics with right angles at that point.

Keywords: Dually flat space, Bregman divergence, geodesic triangle, right angle triangle, Pythagorean theorem, angle excess/defect, Mahalanobis manifold, Itakura-Saito manifold, (extended) Kullback-Leibler manifold, multinoulli manifold.

1 Introduction and motivation

In Euclidean geometry, it is well-known that the sum of the three interior angles of any triangle *always* sum up to π (Figure 1), and that Euclidean triangles can have *at most* one right angle ($\frac{\pi}{2}$ radians or 90°). These facts are not true anymore in hyperbolic geometry nor in spherical geometry [32], where the total sum of the interior angles of a triangle may vary [36]:

- In hyperbolic geometry, hyperbolic triangles have always *angle defects*, meaning that the total sum of the three interior angles of any hyperbolic triangle is always strictly less than π . In the extreme case of hyperbolic ideal triangles, the total sums of their interior angles vanish since the interior angle at an ideal vertex is always 0. Figure 2 displays a right angle hyperbolic triangle and a hyperbolic ideal triangle.
- In spherical geometry, spherical triangles have always *angle excesses*, meaning that the sum of interior angles of any spherical triangle is always strictly greater than π , and is provably upper bounded by 3π radians or 540 degrees. Moreover, there exist spherical triangles with one, two, or three right angles, as depicted in Figure 2.

*This work was published in [21]. This report further contains a section on Bregman balls and Bregman spheres in §2.5.

[†]E-mail: Frank.Nielsen@acm.org. Web: <https://FrankNielsen.github.io/>

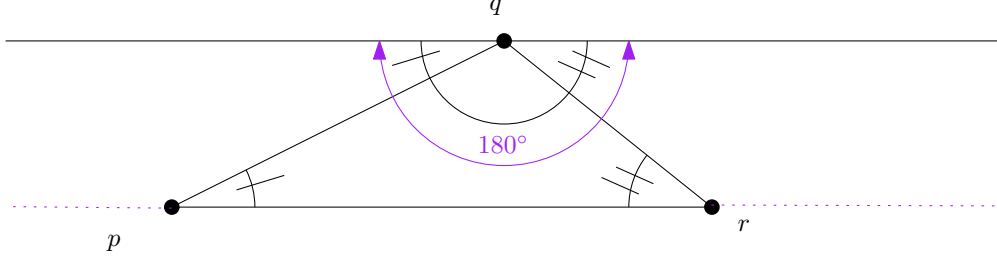


Figure 1: Proof without words: The sum of the three interior angles of any triangle in Euclidean geometry always sum up to π (180 degrees). Euclidean triangles do not show angle defect nor angle excess: The Euclidean space is flat.

More generally, in Riemannian geometry [14], the angle excess or defect of a geodesic triangle reflects the total curvature enclosed by the geodesic triangle via the Gauss-Bonnet formula; The general Gauss-Bonnet formula states that the integral of the scalar curvature of a closed surface is 2π times the Euler characteristic χ of that surface (a topological characteristic). The hyperbolic geometry, Euclidean geometry and spherical geometry can be studied under the framework of Riemannian geometry, as a manifold of constant negative curvature, a flat manifold, and a manifold of constant positive curvature, respectively.

In this work, we consider the *dualistic structure* (M, g, ∇, ∇^*) of information geometry [13, 3] which can be derived from the statistical manifold structure of Lauritzen [16] (M, g, C) : Namely, a simply connected smooth manifold M is equipped with two dual torsion-free affine connections ∇ and ∇^* such that these connections are coupled with the metric tensor g , meaning that their induced dual parallel transport preserves the metric [20]. We shall describe in details that dualistic structure in §2.

Any distinct pair of points p and q on the manifold M can either be joined by a primal ∇ -geodesic arc γ_{pq} or by a dual ∇^* -geodesic arc γ_{pq}^* . Thus any triple of points (p, q, r) of M can be connected pairwise using one of $2 \times \binom{3}{2} = 6$ primal/dual geodesic arcs. Let us parameterize¹ these primal/dual geodesic arcs by $\gamma_{pq}(t)$ and $\gamma_{pq}^*(t)$ so that $\gamma_{pq}(0) = \gamma_{pq}^*(0) = p$ and $\gamma_{pq}(1) = \gamma_{pq}^*(1) = q$. Denote by $v_{pq} := \frac{d}{dt}\gamma_{pq}(t)|_{t=0} = \dot{\gamma}_{pq}(0)$ and $v_{pq}^* := \frac{d}{dt}\gamma_{pq}^*(t)|_{t=0} = \dot{\gamma}_{pq}^*(0)$ the tangent vectors of the tangent plane T_p to the primal and dual geodesics, respectively. Two vectors $u, v \in T_p$ are orthogonal in T_p (denoted notationally by $u \perp_p v$) iff. $g_p(u, v) = 0$:

$$u \perp_p v \Leftrightarrow g_p(u, v) = 0. \quad (1)$$

More generally, two smooth curves $c_1(t)$ and $c_2(t)$ on the manifold are said orthogonal at a point $p = c_1(t_1) = c_2(t_2)$ iff. $g_p(\dot{c}_1(t_1), \dot{c}_2(t_2)) = 0$.

A geodesic triangle T passing through three points $p, q,$ and r (i.e., the triangle vertices) is a triangle with edges linking two vertices defined either by primal or dual geodesic arcs. Thus the dualistic structure of information geometry yields $2^3 = 8$ types of geodesic triangles passing through any three distinct given points p, q and r . Let “p” or \bullet stands for *primal* and “d” or \circ stands for *dual*. A primal geodesic arc γ_{pq} and a dual geodesic arc γ_{pq}^* may also be written γ_{pq}^\bullet and γ_{pq}° , respectively. The 8 types of geodesic triangles are: $\bullet\bullet\bullet$ ppp, $\bullet\bullet\circ$ ppd, $\bullet\circ\bullet$ pdd, $\circ\bullet\bullet$ pdp, $\circ\circ\circ$

¹More precisely, a geodesic $\gamma_{pq}^\nabla(t)$ with respect to an affine connection ∇ satisfies $\nabla_{\dot{\gamma}_{pq}} \dot{\gamma}_{pq} = 0$. A ∇ -geodesic is an autoparallel curve as it is invariant by affine reparameterization of t (i.e., $t' = at + b$).

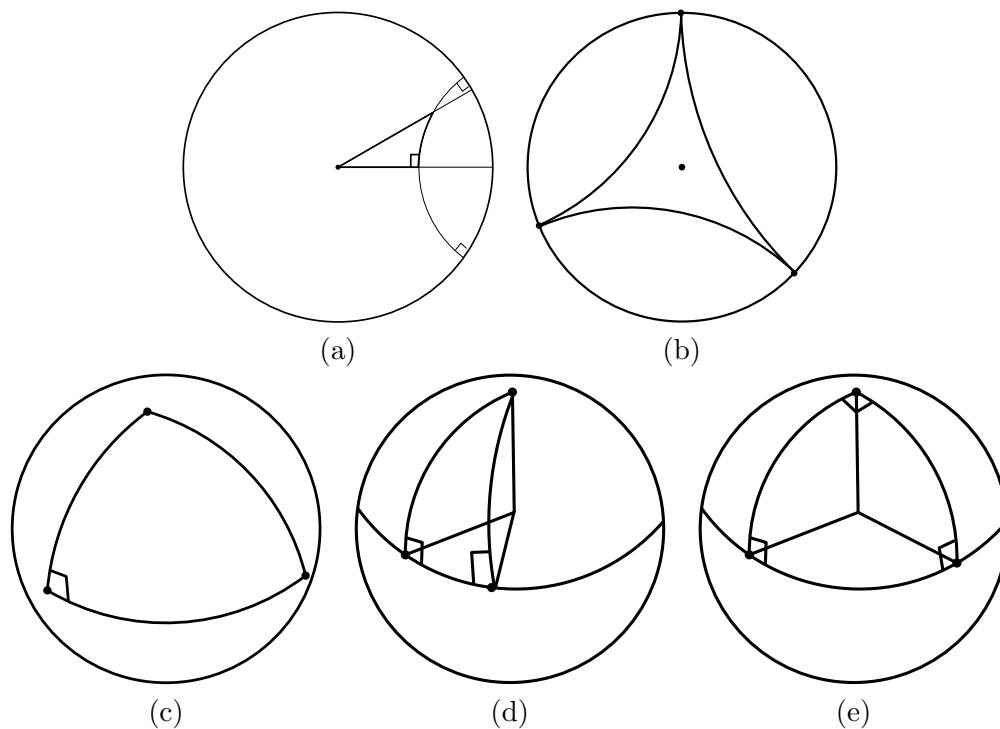


Figure 2: In hyperbolic geometry, triangles have angle defects: Visualization in the Poincaré conformal disk model. (a) hyperbolic triangle with one right angle, (b) hyperbolic ideal triangle with all interior angles equal to zero (and area always π). In spherical geometry, triangles have angle excesses: Visualization of spherical triangles on the unit 3D sphere. (c) spherical triangle with one right angle, (d) spherical triangle with two right angles, and (e) spherical triangle with three right angles.

Geodesic triangle T	Dual geodesic triangle T^*
$T = \gamma_{pq}\gamma_{qr}\gamma_{rp}$ (type $\bullet\bullet\bullet$ ppp : a ∇ -triangle)	$T^* = \gamma_{pq}^*\gamma_{qr}^*\gamma_{rp}^*$ (type $\bullet\bullet\bullet$ ddd: a ∇^* -triangle)
$T = \gamma_{pq}\gamma_{qr}\gamma_{rp}^*$ (type $\bullet\bullet\bullet$ ppp)	$T^* = \gamma_{pq}^*\gamma_{qr}^*\gamma_{rp}$ (type $\bullet\bullet\bullet$ ddd)
$T = \gamma_{pq}\gamma_{qr}^*\gamma_{rp}$ (type $\bullet\bullet\bullet$ ppp)	$T^* = \gamma_{pq}^*\gamma_{qr}\gamma_{rp}$ (type $\bullet\bullet\bullet$ ddd)
$T = \gamma_{pq}\gamma_{qr}^*\gamma_{rp}^*$ (type $\bullet\bullet\bullet$ ppp)	$T^* = \gamma_{pq}^*\gamma_{qr}\gamma_{rp}^*$ (type $\bullet\bullet\bullet$ ddd)
$T = \gamma_{pq}\gamma_{qr}^*\gamma_{rp}$ (type $\bullet\bullet\bullet$ ppp)	$T^* = \gamma_{pq}^*\gamma_{qr}\gamma_{rp}$ (type $\bullet\bullet\bullet$ ddd)
$T = \gamma_{pq}\gamma_{qr}^*\gamma_{rp}$ (type $\bullet\bullet\bullet$ ppp)	$T^* = \gamma_{pq}^*\gamma_{qr}\gamma_{rp}$ (type $\bullet\bullet\bullet$ ddd)

Table 1: Eight types of geodesic triangles paired by duality.

ddd, $\bullet\bullet\bullet$ ddp, $\bullet\bullet\bullet$ dpp, and $\bullet\bullet\bullet$ dpd. We can group these eight types of geodesic triangles into two groups of four geodesic triangles each as shown in Table 1.

A geodesic triangle T^* is dual to another geodesic triangle T iff. each geodesic arc of T^* is corresponding to a dual geodesic arc of T . For example, the triangle $T^* = \gamma_{pq}^*\gamma_{qr}\gamma_{rp}$ (type $\bullet\bullet\bullet$ dpp) is dual to the triangle $T = \gamma_{pq}\gamma_{qr}^*\gamma_{rp}$ (type $\bullet\bullet\bullet$ ppp). At each triangle vertex, we have 4 geodesic arcs defining $\binom{4}{2} = 6$ angles. A triple of points defines 8 geodesic triangles with $4 \times 3 = 12$ interior angles.² The interior angle $\alpha_p(c_{pq}, c_{pr})$ of a geodesic triangle $T = c_{pq}c_{qr}c_{rp}$ (where c_{ab} stands either for γ_{ab} or for γ_{ab}^*) at p is measured according to the metric tensor g as follows:

$$\alpha_p(c_{pq}, c_{pr}) = \arccos \left(\frac{g_p(\dot{c}_{pq}(0), \dot{c}_{pr}(0))}{\|\dot{c}_{pq}(0)\|_p \|\dot{c}_{pr}(0)\|_p} \right) = \alpha_p(c_{pr}, c_{pq}), \quad (2)$$

where $\|v\|_p = \sqrt{g_p(v, v)}$ measures the length of vector $v \in T_p$. The total sum $\alpha(T)$ of the three interior angles of a geodesic triangle $T = c_{pq}c_{qr}c_{rp}$ is defined by

$$\alpha(T) := \alpha_p(c_{pq}, c_{pr}) + \alpha_q(c_{qp}, c_{qr}) + \alpha_r(c_{rp}, c_{rq}). \quad (3)$$

We may specify a geodesic triangle as follows: $T_E(p, q, r)$ where $p, q, r \in M$ are the three triangle vertices (points on M), and $E \in (t_1 \in \{p, d\}, t_2 \in \{p, d\}, t_3 \in \{p, d\})$ is the type of primal/dual geodesic edges of the triangle so that $c_{ab}^{t_i} = \gamma_{ab}$ if $t_i = p$ and $c_{ab}^{t_i} = \gamma_{ab}^*$ if $t_i = d$. A geodesic triangle $T = T_E(p, q, r)$ with all primal geodesics arcs ($E = (p, p, p)$) is called a ∇ -triangle, and its dual geodesic triangle $T^* = T_{E^*}(p, q, r)$ (with all dual geodesic arcs, i.e., $E^* = (d, d, d)$) is called a ∇^* -triangle.

By considering duality of geodesic triangles and permutations of the triple of points p, q and r , we may reduce the study of interior angles between a pair of geodesics at a vertex to three types of primal geodesic triangles (type ppp, pdp, and pdd) with their corresponding dual geodesic triangles (type ddd, dpd and dpp, respectively).

A particular case of information-geometric manifolds are *dually flat spaces* [3] induced by a strictly convex and C^3 function F called the *potential function*. In a dually flat space M , there are two global dual affine coordinate systems θ and η (with $M = \{p : \theta(p) \in \text{dom}(F)\}$), and a generalization of the Pythagoras' theorem holds [3]. The divergence $D_F(p : q)$ (potentially oriented distance, $D_F(p : q) \neq D_F(q : p)$) between two points p and q can be expressed using the Bregman divergence B_F on their primal coordinates:

$$D_F(p : q) = B_F(\theta(p) : \theta(q)) = F(\theta(p)) - F(\theta(q)) - (\theta(p) - \theta(q))^\top \nabla F(\theta(q)). \quad (4)$$

²We do consider at a triangle vertex only pairs of geodesics with interior angles linking the two other triangle vertices.

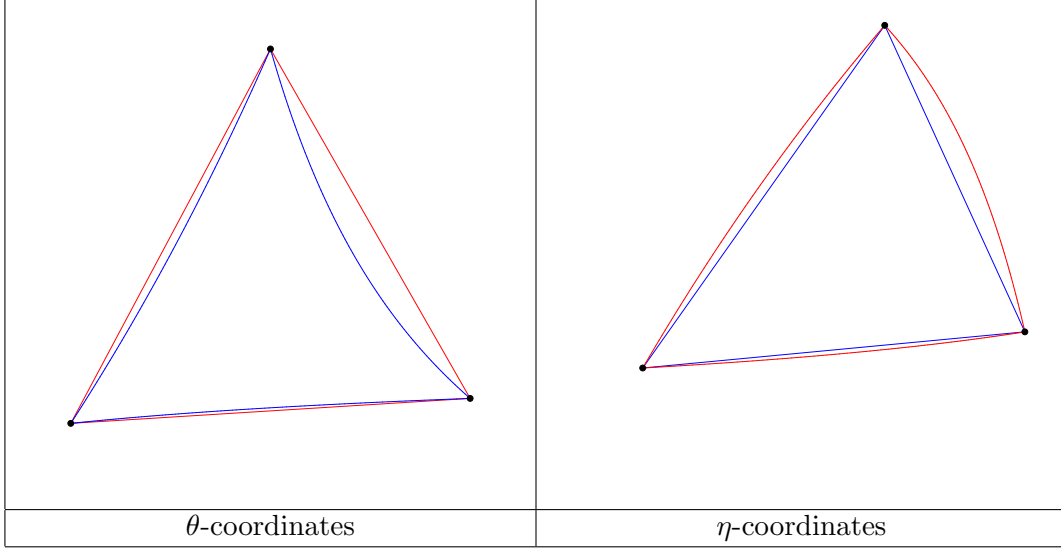


Figure 3: The $2 \times 3 = 6$ potential geodesic arcs (edges) of a geodesic triangle T visualized both in the primal θ -coordinate system (left) and in the dual η -coordinate system (right). The vertices are $\theta(p) = (0.55, 0.575)$, $\theta(q) = (0.75, 0.95)$ and $\theta(r) = (0.95, 0.6)$ for the Bregman manifold defined by the 2D Burg negentropy: $F_{\text{Burg}}(\theta^1, \theta^2) = -\log(\theta^1) - \log(\theta^2)$. Primal geodesic arcs are shown in red and are visualized as straight line segments in the θ -coordinate system. Dual geodesic arcs are shown in blue and are visualized as straight line segments in the η -coordinate system.

Whenever it is clear from context, we shall write D instead of D_F for conciseness.

Since the canonical divergence of a dually flat space (M, g, ∇, ∇^*) amounts to a Bregman divergence [3], we shall also call these dually flat spaces *Bregman manifolds* (M, F) in the remainder. When the Bregman generator is $F_{\text{Euc}}(\theta) = \frac{1}{2}\theta^\top \theta$, we recover the Euclidean geometry (a self-dual Bregman manifold) where the *Euclidean divergence* is half of the squared of the Euclidean distance. Beware that the Euclidean distance is a metric distance but the Euclidean divergence is not.

Figure 4 displays the 8 types of geodesic triangles in a Bregman manifold obtained for the 2D generator $F_{\text{Burg}}(\theta) = -\log \theta^1 - \log \theta^2$ (called Burg negentropy [27]) with corresponding Bregman divergence called the Itakura-Saito divergence [27, 6].

In this paper, we raise and (partially) answer the following questions on a statistical manifold:

- Q1.** When and how can one build geodesic triangles with one, two and three right angles?
- Q2.** When and how can one build dual geodesic triangles T and T^* such that at a triangle vertex, we have two pairs of dual geodesics emanating from that vertex that are simultaneously orthogonal?
- Q3.** When is there a relationship or inequality between $\alpha(T)$ and $\alpha(T^*)$?

In this work, we are interested in studying these questions and unraveling some properties of geodesic triangles in the particular case of dually flat spaces, Bregman manifolds. In Bregman manifolds, the Pythagorean theorem allows one to check that a pair of dual geodesics is orthogonal at a given point by checking some divergence identity. In general, the Pythagorean theorem is useful to prove uniqueness of projections in particular settings, interpret geometrically projections

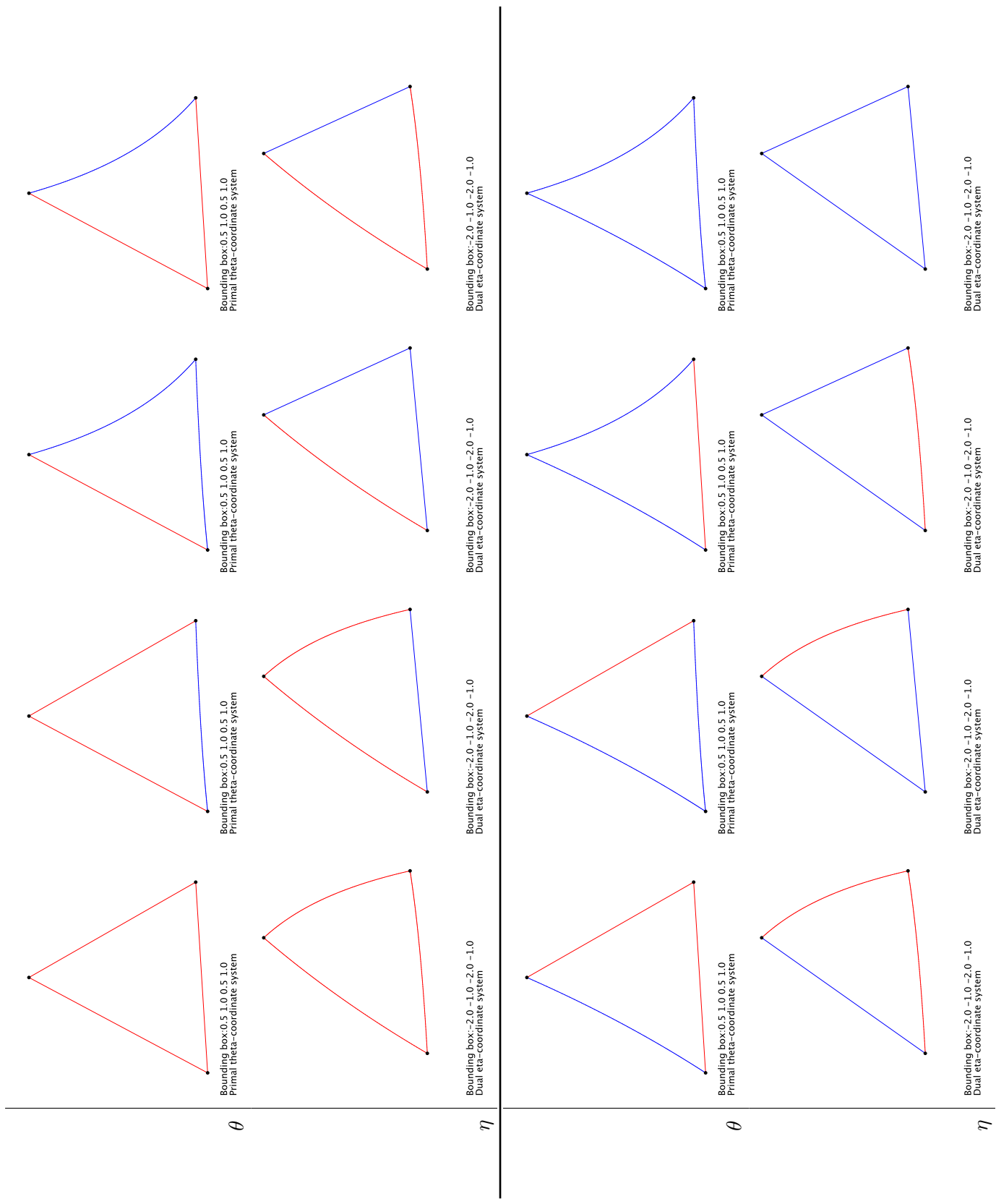


Figure 4: The $2^3 = 8$ types of geodesic triangles visualized both in the primal θ -coordinate system and the dual η -coordinate system. Primal geodesic edges are shown in red and are straight in the θ -coordinate system. Dual geodesic edges are shown in blue and are straight in the η -coordinate system. Refer to Figure 3 for point coordinates.

based on the divergence, and design derivative-free projection algorithms [1]. In information geometry, besides the dually flat spaces, Pythagorean theorems with corresponding divergence identities have also been reported for α -divergences on the probability simplex [3] and the logarithmic L_H^α -divergences [37] where H is an exponentially concave generator.

The paper is organized as follows: First, we quickly review the construction of Bregman manifolds in §2, thereby introducing familiar concepts and notations of information geometry [3], and give as examples of Bregman manifolds details for the Mahalanobis manifolds (§2.4.1), the extended Kullback-Leibler manifold (§2.4.2), the Itakura-Saito manifold (§2.4.3), and the multinoulli manifolds (§2.4.4). Then Section 3 shows, whenever it is possible, how to build geodesic ∇ -triangles which have one, two or three right angles (thus necessarily exhibiting angle excesses for two and three right angle triangles). In §4, we prove that given two distinct points p and q , the loci of points r for which we have simultaneously the dual Pythagorean theorems holding at r are the intersection of an autoparallel ∇ -submanifold with an autoparallel ∇^* submanifold (i.e., the intersection of a θ -flat with a η -flat [3]). We report explicitly the construction method for the 2D Itakura-Saito manifold and visualize several such triangles. Finally, we summarize and hint at further perspectives in §5.

2 Dually flat spaces: Bregman manifolds

We first explain the mutually orthogonal primal basis and reciprocal basis in an inner product space in §2.1. Then we describe dual geodesics and their tangent vectors and the dual parallel transport in §2.2. In §2.3, we explain the Pythagorean theorem, and §2.4 provides some common examples of Bregman manifold: Mahalanobis self-dual manifolds, the extended Kullback-Leibler manifold and the Itakura-Saito manifold.

2.1 Preliminary: inner product space and reciprocal basis

An *inner product space* is a vector space V equipped with a symmetric positive definite bilinear form $\langle \cdot, \cdot \rangle : V \times V \rightarrow \mathbb{R}$ called the inner product. The length of a vector $v \in V$ is given by its induced norm $\|v\| = \sqrt{\langle v, v \rangle}$, and the angle between any two vectors u and v is measured as $\alpha(u, v) = \arccos\left(\frac{\langle u, v \rangle}{\|u\|\|v\|}\right)$ (in radians). We consider finite D -dimensional inner product spaces where a vector v can be expressed in *any* basis $B = \{e_1, \dots, e_D\}$ (a maximum set of linearly independent vectors) by its components $v_B = (v^1, \dots, v^D)$: $v = \sum_{i=1}^D v^i e_i$. Vector v can also be expressed equivalently in an other basis $\hat{B} = \{\hat{e}_1, \dots, \hat{e}_D\}$: $v = \sum_{i=1}^D \hat{v}^i \hat{e}_i$. Notice that in general the components v_B and $v_{\hat{B}}$ are different although they express the same geometric vector v according to their respective basis B and \hat{B} . We can express the basis vectors \hat{e}_i using basis B and the basis vectors e_i using basis \hat{B} as $\hat{e}_i = \hat{A}_i^j e_j$ and $e_j = A_j^i \hat{e}_i$, respectively (using Einstein summation convention). We have $\hat{A}_i^j A_j^k = \delta_i^k$ where δ_i^j is the Kröner symbol ($\delta_i^j = 1$ iff. $i = j$ and 0 otherwise), and the changes of basis reflects on components as $v^i = \hat{A}_j^i \hat{v}^j$ and $\hat{v}^i = A_j^i v_j$. When the basis B is orthonormal (i.e., $\langle e_i, e_j \rangle = \delta_{ij}$ where δ_{ij} is the Kröner symbol: $\delta_{ij} = 1$ iff. $i = j$ and 0 otherwise) the vector components can be retrieved from the inner product as $v^i = \langle v, e_i \rangle = \langle \sum_{j=1}^D v^j e_j, e_i \rangle = \sum_{j=1}^D v^j \langle e_j, e_i \rangle$. This is no longer true for non-orthormal basis (e.g., an orthogonal but non-orthonormal basis or an oblique basis). Let us introduce the unique *reciprocal basis* $B^* = \{e^{*1}, \dots, e^{*D}\}$ such that by construction, we have $\langle e_i, e^{*j} \rangle = \delta_i^j$. The vector v can be

expressed in the reciprocal basis as $v = \sum_{i=1}^D v_i e^{*i}$. The vector components v^i (superscript notation) wrt. basis B are called the *contravariant components*, and $v^i = \langle v, e^{*i} \rangle$. The vector components v_i (subscript notation) wrt. basis B^* are called the *covariant components*, and $v_i = \langle v, e_i \rangle$. (We shall explain this contravariant/covariant component terminology at the end of this section.)

Let $G = [g_{ij} = \langle e_i, e_j \rangle]_{ij}$ and $G^* = [g^{*ij} = \langle e^{*i}, e^{*j} \rangle]_{ij}$ denote the $D \times D$ positive definite matrices, called dual metrics. These dual metric matrices are inverse of each other: $G^* = G^{-1}$. In textbooks, one often drops the superscript star $*$ in the notation of the reciprocal basis and the dual riemannian metric, see [3]. Here, we keep them explicitly for easing the understanding, even if they load the notations.

We can convert the contravariant components v^i of a vector v to its covariant components v_i , and vice versa, using these metric matrices: $v_i = \sum_{j=1}^D g_{ij} v^j$ and $v^i = \sum_{j=1}^D g^{*ij} v_j$. Let $[u]_B$ denote the vector components of u in basis B arranged in a column vector. Then we rewrite the contravariant/covariant conversions as matrix-vector multiplications of linear algebra: $[v]_{B^*} = G \times [v]_B$ and $[v]_B = G^* \times [v]_{B^*}$. The inner product between two vectors can be written equivalently using algebra as

$$\langle u, v \rangle = \sum_{i=1}^D u_i v^i = [u]_{B^*}^\top \times [v]_B, \quad (5)$$

$$= \sum_{i=1}^D u^i v_i = [u]_B^\top \times [v]_{B^*}, \quad (6)$$

$$= \sum_{i=1}^D [u]_B^\top \times G^* \times [v]_B, \quad (7)$$

$$= \sum_{i=1}^D [u]_{B^*}^\top \times G \times [v]_{B^*}. \quad (8)$$

In differential geometry [3, 20], a smooth manifold M is equipped with a *metric tensor field* g that defines on each tangent plane T_p of $p \in M$ an inner product. The dual of a tangent plane T_p is the cotangent plane T_p^* , a vector space of linear functionals. In general, tensor fields define at each point of the manifold component-free geometric entities that can be interpreted as multilinear functionals over Cartesian products of dual covector and vector spaces. A vector v of T_p is a rank-1 tensor that can be expressed either using the covariant or contravariant components of a reciprocal basis. Thus one should not confuse the notion of “geometric vectors” that are tensors (coordinate-free objects independent of the choice of the basis) with the “column vectors” of vector components in a basis which are used to perform linear algebra calculations on (geometric) vectors. When the components of a tensor vector varies with the inverse transformation of the change of basis, we say that we have a contravariant (tensor) vector (a $(0, 1)$ -tensor), and its components are called contravariant components. When the components of a tensor vector varies according to the transformation of the change of basis, we say that we have a covariant (tensor) vector (a covector or $(1, 0)$ -tensor, i.e., an element of the dual vector space V^* of linear functionals or linear forms), and its components are called covariant components. The metric tensor g is a $(2, 0)$ covariant tensor [20].

2.2 Dual geodesics and their tangent vectors, and dually coupled parallel transport

Let $F(\theta)$ be a D -dimensional C^3 real-valued function defined on an *open* convex domain Θ , and denote by $F^*(\eta)$ its Legendre-Fenchel convex conjugate [3, 20]: $F^*(\eta) = \sup_{\theta \in \Theta} \theta^\top \eta - F(\theta)$. The dual potential functions F and F^* induce two torsion-free flat affine connections [20] ∇ and ∇^* , respectively. A Bregman manifold M is equipped with two global affine coordinate systems $\theta(\cdot)$ (the ∇ -affine coordinate system) and $\eta(\cdot)$ (the ∇^* -affine coordinate system) such that it comes from Legendre-Fenchel transformation that $\eta(\theta) = \nabla F(\theta)$ and $\theta(\eta) = \nabla F^*(\eta)$. Let $\theta^i(p)$ and $\eta_i(p)$ denote the primal i -th θ -coordinate functions and the dual i -th η -coordinate functions of a point p , for $i \in \{1, \dots, D\}$ so that $\theta(p) = (\theta^1(p), \dots, \theta^D(p))$ and $\eta(p) = (\eta_1(p), \dots, \eta_D(p))$. Notations are summarized in Appendix A. Any point $p \in M$ can be expressed equivalently either in the primal global θ -chart or the dual global η -chart. The dual geodesics³ γ_{pq} and γ_{pq}^* passing through two given points $p, q \in M$ write simply using the dual coordinate systems as follows:

$$\gamma_{pq} = \{x_\lambda \in M : \theta(x_\lambda) = (1 - \lambda)\theta(p) + \lambda\theta(q), \quad \lambda \in [0, 1]\}, \quad (9)$$

$$\gamma_{pq}^* = \{x_\lambda \in M : \eta(x_\lambda) = (1 - \lambda)\eta(p) + \lambda\eta(q), \quad \lambda \in [0, 1]\}. \quad (10)$$

In general, a vector field $v(t)$ is parallel along a smooth curve $c(t)$ iff.

$$\forall i \in \{1, \dots, D\}, \quad \dot{v}^i + \sum_{j,k=1}^D \Gamma_{jk}^i \dot{x}^j v^k = 0. \quad (11)$$

Since the Christoffel symbols $\Gamma_{jk}^i(\theta) = 0$ (and $\Gamma_{jk}^{*i}(\eta) = 0$) in a dually flat space, we have $\dot{v}^i = 0$ and recover the equation of the primal geodesic (and $\dot{v}_i = 0$ for the equation of the dual geodesic, respectively).

The dual Riemannian metrics $[g_{ij}] = [g_{ji}]$ and $[g^{*ij}] = [g^{*ji}]$ are induced by the Hessians of the dual potential functions F and F^* (both symmetric positive-definite matrices), respectively. At any given point $p \in M$, we consider the natural basis $\{e_i = \partial_i = \frac{\partial}{\partial \theta^i}\}$ and the reciprocal basis $\{e^{*i} = \partial^i = \frac{\partial}{\partial \eta_i}\}_i$ of the tangent plane T_p so that $g(e_i, e^{*j}) = \delta_i^j$. That is, the basis vectors of the primal and reciprocal basis are *mutually orthogonal*. We have $[g_{ij}] = [g(e_i, e_j)]_{ij} = \nabla^2 F(\theta)$ and $[g^{*ij}] = [g^*(e^{*i}, e^{*j})]_{ij} = \nabla^2 F^*(\eta)$. We can check that the natural primal basis and the dual reciprocal basis are mutually orthogonal from Crouzeix identity:

$$\nabla^2 F(\theta) \nabla^2 F^*(\eta) = I, \quad (12)$$

where I denotes the $D \times D$ identity matrix. Note that Eq. 12 can be read using a single coordinate system as $\nabla^2 F(\theta) \nabla^2 F^*(\eta(\theta)) = \nabla^2 F(\theta) \nabla^2 F^*(\nabla F(\theta)) = I$ or $\nabla^2 F(\theta(\eta)) \nabla^2 F^*(\eta) = \nabla^2 F(\nabla F^*(\eta)) \nabla^2 F^*(\eta) = I$.

A tangent vector v_{pq} of the primal geodesic γ_{pq} at p is a vector of the tangent plane T_p with contravariant components $\theta(q) - \theta(p)$ (say, expressed in the primal basis $B_p = \{e_1, \dots, e_D\}$): $v = \sum_{i=1}^D (\theta^i(q) - \theta^i(p)) e_i$ with $v^i = \theta^i(q) - \theta^i(p)$. Indeed, we have

$$\frac{d\gamma_{pq}(t)}{dt} = \frac{d}{dt} ((1-t)\theta(p) + t\theta(q)) = \sum_i (\theta^i(q) - \theta^i(p)) \partial_i, \quad (13)$$

³Given an affine connection ∇ , the ∇ -geodesic is an autoparallel curve [20].

where $\partial_i = \frac{\partial}{\partial \theta^i}$. Similarly, a tangent vector v_{pq}^* at the dual geodesic γ_{pq}^* is a vector of the tangent plane T_p with covariant components $\eta(q) - \eta(p)$ (expressed in the reciprocal basis $B_p^* = \{e^{*1}, \dots, e^{*D}\}$): $v = \sum_{i=1}^D (\eta_i(q) - \eta_i(p)) e^{*i}$. Indeed, we check that

$$\frac{d\gamma_{pq}^*(t)}{dt} = \frac{d}{dt} ((1-t)\eta(p) + t\eta(q)) = \sum_i (\eta_i(q) - \eta_i(p)) \partial^i, \quad (14)$$

where $\partial^i = \frac{\partial}{\partial \eta_i}$. In general, for separable Bregman generators, i.e., $F(\theta) = \sum_{i=1}^D F_i(\theta^i)$ where the F_i 's are scalar strictly convex and C^3 functions, we can choose both the primal and reciprocal basis to be orthogonal but they are not necessarily orthonormal (except in the special case of the Euclidean geometry obtained by $F(\theta) = \sum_{i=1}^D \text{sqr}(\theta^i)$ where $\text{sqr}(x) := x^2$ denotes the square function).

The metric tensor field g defines a smooth scalar product $g(\cdot, \cdot)$ on the tangent bundle TM (informally, the union of all tangent planes) such that for any two vectors $u, v \in T_p$, we have $g_p(u, v) = u_i v^i = u^i v_i$. In each tangent plane, we thus have an inner product space. The contravariant and covariant components of a vector v can be retrieved using the inner product with the reciprocal basis and the primal basis, respectively: $v^i = g(v, e^{*i})$, and $v_i = g(v, e_i)$. We can also use vector-matrix multiplications of linear algebra to calculate the inner product: $g_p(u, v) = [u^i]^\top \times \nabla^2 F(\theta(p)) \times [v^i] = [u_i]^\top \times \nabla^2 F^*(\eta(p)) \times [v_i]$, where $[u^i]$ and $[u_i]$ denote the column-vector of the contravariant components of u and covariant components of u , respectively. Since $v^i = \nabla^2 F^*(\eta(p)) \times [v_i]$ and $v_i = \nabla^2 F(\theta(p)) \times [v^i]$, we therefore have the following equivalent rewritings of the inner product:

$$g_p(u, v) = [u_i]^\top \times [v^i], \quad (15)$$

$$= [u^i]^\top \times [v_i], \quad (16)$$

$$= [u^i]^\top \times \nabla^2 F(\theta(p)) \times [v^i], \quad (17)$$

$$= [u_i]^\top \times \nabla^2 F^*(\eta(p)) \times [v_i]. \quad (18)$$

When the generator $F(\theta)$ is separable, i.e., $F(\theta) = \sum_{i=1}^D F_i(\theta^i)$ for univariate generators F_i 's, the inner product at a tangent plane T_p writes equivalently as (using Einstein summation convention):

$$g_p(u, v) = u^i F_i''(\theta^i(p)) v^i, \quad (19)$$

$$= u_i F_i^{*''}(\eta_i(p)) v_i, \quad (20)$$

$$= u_i v^i, \quad (21)$$

$$= u^i v_i. \quad (22)$$

Given two vectors $u, v \in T_p$, we measure their lengths $\|u\|_p$ and $\|v\|_p$ and the interior angle $\alpha_p(u, v)$ between them as:

$$\|u\|_p = \sqrt{g_p(u, u)} = \sqrt{u^i u_i}, \quad (23)$$

$$\|v\|_p = \sqrt{g_p(v, v)} = \sqrt{v^i v_i}, \quad (24)$$

$$\alpha_p(u, v) = \arccos \left(\frac{u^i v_i}{\|u\|_p \|v\|_p} \right) = \alpha_p(v, u). \quad (25)$$

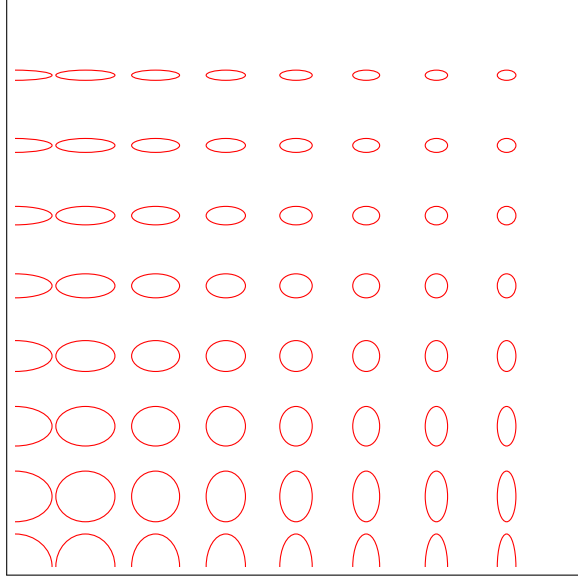


Figure 5: Visualization of the metric tensor field $g(\theta) = \text{diag}\left(\frac{1}{\text{sqr}(\theta^1)}, \frac{1}{\text{sqr}(\theta^2)}\right)$ for the 2D Itakura-Saito manifold. The metric tensor field g is not conformal. This can be seen from ellipses depicting the metric tensors (tiny Bregman circles) at regularly sampled grid positions which are not scaled (Euclidean) circles.

Notice that the Hessian metric g and g^* are not conformal (i.e., not a positive scalar function of the Euclidean metric), and that we cannot “read” the angles directly in the θ - or η -coordinate systems. In other words, the Euclidean angles displayed in the θ - or η -coordinate systems do not correspond to the intrinsic angles of the underlying Bregman geometry. Figure 5 shows a visualization of the metric tensor field for the Itakura-Saito manifold (with $[g_{ij}](\theta) = \nabla^2 F(\theta) = \text{diag}(\frac{1}{\text{sqr}(\theta^1)}, \frac{1}{\text{sqr}(\theta^2)})$ for 2D $\theta = (\theta^1, \theta^2)$). Dually flat spaces are a particular case of more general (local) Hessian structures studied in [34].

In information geometry [3], the dually flat torsion-free affine connections⁴ ∇ and ∇^* are coupled the metric tensor g . An affine connection ∇ is flat iff. there exists a coordinate system such that its Christoffel symbols Γ expressed in a coordinate system vanishes. For Bregman manifolds, we have both $\Gamma_{ijk}(\theta) = 0$ and $\Gamma^{*ijk}(\eta) = 0$, see [3], so the connections ∇ and ∇^* are both flat. Notice that a cylinder is ∇ -flat for the natural Euclidean connection but geodesic triangles on the cylinder have interior angles not summing up to π . That is, let $\mathcal{X}(M)$ denotes the space of smooth vector fields (the cross sections of the tangent bundles TM). We say that the two torsion-free affine connections ∇ and ∇^* are dual when it holds that

$$\forall X, Y, Z \in \mathcal{X}(M), \quad Xg(Y, Z) = g(\nabla_X Y, Z) + g(Y, \nabla_X^* Z). \quad (26)$$

An important consequence of the coupling of the dual connections to the metric is that the dual parallel transport preserves the metric.

Let us choose by convention to fix the primal basis of the tangent vectors at T_p for any $p \in M$

⁴The notion of dual connections of information geometry is more general than the notion of conjugate connections of affine differential geometry [15] which stems from dual affine immersions.

to be the e_i 's, the one-hot vectors in the θ -coordinate system, i.e., $e_i = (\underbrace{0, \dots, 0}_{i-1}, 1, 0, \dots, 0)$ (the standard basis of \mathbb{R}^D). This is the canonical basis.⁵ Since the ∇ -connection is flat, the primal parallel transport $\prod_{p,q}(v)$ of a vector v of T_p to a corresponding vector T_q is *independent* of the chosen smooth curve, and we have for $v = \sum_i v^i e_i|_p \in T_p$

$$\prod_{p,q}(v) = v^i e_i|_q \in T_q. \quad (27)$$

That is, the contravariant components of v do not change with primal parallel transport assuming that the primal basis is fixed for all tangent planes, i.e., $B_q = B_p, \forall p, q \in M$ (and $e_i|_p = e_i|_q$).

Similarly, since the ∇^* -connection is flat, the dual parallel transport $\prod_{p,q}^*(v)$ of a vector v of T_p to a corresponding vector of T_q is independent of the chosen smooth curve, and we have

$$\prod_{p,q}^*(v) = v_i e^{*i}|_q. \quad (28)$$

However, because $B_q^* = \{e^{*i}|_q\}$ is the reciprocal basis of the fixed primal basis $B_q = \{e_i|_q\} = e_i$, the basis B_q^* varies accordingly to the metric tensor g (and $B_q^* \neq B_p^*$). Indeed, in general, we cannot fix both the primal and reciprocal basis in all tangent planes because they relate to each other by construction by the metric tensor. This is only possible when $G(\theta(p)) = G^*(\eta(p)) = I$, the $D \times D$ identity matrix, corresponding to the special case of Euclidean or Mahalanobis geometry.

Let us now check the metric compatibility of the dual parallel transport of two vectors $u, v \in T_p$ to T_q :

$$g_q \left(\prod_{p,q}(u), \prod_{p,q}^*(v) \right) = g_p(u, v). \quad (29)$$

Proof. We have

$$g_q \left(\prod_{p,q}(u) = u^i e_i|_q, \prod_{p,q}^*(v) = v_i e^{*i}|_q \right) = u^i v_i g_q \left(e_i|_q, e^{*i}|_q \right), \quad (30)$$

$$= u^i v_i, \quad (31)$$

$$= u^i v_i g_p \left(e_i|_p, e^{*i}|_p \right), \quad (32)$$

$$= g_p(u, v). \quad (33)$$

□

Figure 6 displays the parallel transport of the tangent vector $\dot{\gamma}_{pq}^*(0)$ from T_p to $T_{\gamma_{pq}^*(t)}$ for several time steps t . Although the dual parallel transport preserves the metric, the length of a vector transported by either the primal or the dual parallel transport varies.

Historically, the dual parallel transport coupled to the metric tensor was studied independently by Norden [31] and Sen [33] in the 1930's and 1940's, respectively.

⁵In differential geometry, the tangent plane at a point p is the space of all linear derivations that satisfies the Leibniz's rule. A basis $\{t_i\}_i$ of T_p is such that $t_i(f) = \frac{\partial f}{\partial \theta^i}$.

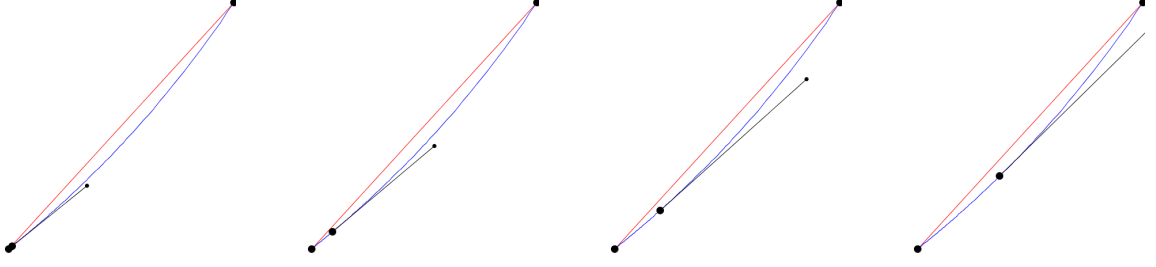


Figure 6: Dual parallel transport of tangent vector $\dot{\gamma}_{pq}^*(0)$ at T_p along the ∇^* -geodesic: Since the dual geodesic $\gamma_{pq}^*(t)$ is a ∇^* -autoparallel curve, the tangent vector at $\dot{\gamma}_{pq}^*(0)$ is transported into tangent vectors along that dual geodesic.

2.3 Dual Pythagorean theorems

The divergence $D_F(p : q)$ from a point p to a point q can be expressed using dual Bregman divergences as follows:

$$D_F(p : q) = B_F(\theta(p) : \theta(q)) = D^*(q : p) = B_{F^*}(\eta(q) : \eta(p)), \quad (34)$$

where $D_F^*(p : q) := D_F(q : p)$ denotes the reverse divergence, and

$$B_F(\theta_1 : \theta_2) = F(\theta_1) - F(\theta_2) - (\theta_1 - \theta_2)^\top \nabla F(\theta_2), \quad (35)$$

is the Bregman divergence associated to generator F . Bregman divergences generalize the squared Euclidean distance with the relative entropy, and thus offer a nice framework to unify or develop generic algorithms [5]. Bregman divergences proved useful in machine learning [6] and topological data analysis [12] among others.

Now, consider two smooth curves $c_1(t)$ and $c_2(t)$ intersecting at a point $p = c_1(0) = c_2(0)$. Denote by $\dot{c}_1(0) = \frac{d}{dt}c_1(t)|_{t=0}$ and $\dot{c}_2(0) = \frac{d}{dt}c_2(t)|_{t=0}$ the tangent vectors to the curves at point p , belonging to the tangent plane T_p . Curve c_1 is said *orthogonal* to curve c_2 at p , i.e., $c_1(t) \perp_p c_2(t)$, iff. $g_p(\dot{c}_1(0), \dot{c}_2(0)) = 0$.

In a Bregman manifold, the remarkable following generalized Pythagorean theorem holds:

Theorem 1 (Generalized Pythagorean theorem) *When a primal geodesic γ_{pq} is orthogonal to a dual geodesic γ_{qr}^* at point q (i.e., $\gamma_{pq} \perp_q \gamma_{qr}^*$), we have $(\theta(p) - \theta(q))^\top (\eta(r) - \eta(q)) = 0$, and the following Pythagorean divergence identity holds:*

$$D_F(p : q) + D_F(q : r) = D_F(p : r). \quad (36)$$

Proof. The proof proceeds in two steps:

- First, Let us show that the test $(\theta(p) - \theta(q))^\top (\eta(r) - \eta(q)) = 0$ can be rewritten as an inner product showing that

$$(\theta(p) - \theta(q))^\top (\eta(r) - \eta(q)) = g_q(v_{qp}, v_{qr}^*) = g_q(\dot{\gamma}_{qp}(0), \dot{\gamma}_{qr}^*(0)), \quad (37)$$

where v_{pq} denotes the tangent vector at q of the primal geodesic γ_{pq} , and v_{qr}^* is the tangent vector at q of the dual geodesic γ_{qr}^* . Indeed, the inner product is $g(v_{qp}, v_{qr}^*) = (v_{qp})^i (v_{qr}^*)_i$ and we have

$$(\theta(p) - \theta(q))^\top (\eta(r) - \eta(q)) = [\theta_{pq}]^\top \times \nabla^2 F(\theta(q)) (\nabla^2 F(\theta(q)))^{-1} \times [\eta_{rq}^*], \quad (38)$$

where $\theta_{pq} := \theta(p) - \theta(q)$ (contravariant components of v_{qp}) and $\eta_{rq}^* := \eta(r) - \eta(q)$ (covariant components of v_{qr}^*). That is, $[(v_{qp})^i] = \theta_{pq}$ and $[v_{qr}^*]_i = \eta_{pq}$. Using the Crouzeix identity [9] of Eq. 12, we get

$$(\theta(p) - \theta(q))^\top (\eta(r) - \eta(q)) = [\theta_{pq}]^\top \nabla^2 F(\theta(q)) (\nabla^2 F^*(\eta(q))) [\eta_{rq}^*]. \quad (39)$$

The term $(\nabla^2 F^*(\eta(q))) \times [\eta_{rq}^*]$ gives the contravariant components θ_{rq}^* of the vector v_{qr}^* . Thus we have checked that

$$(\theta(p) - \theta(q))^\top (\eta(r) - \eta(q)) = [\theta_{pq}]^\top \times \nabla^2 F(\theta(q)) \times [\theta_{rq}^*] = g_q(v_{qp}, v_{qr}^*). \quad (40)$$

That is,

$$(\theta(p) - \theta(q))^\top (\eta(r) - \eta(q)) = 0 \Leftrightarrow \dot{\gamma}_{pq}(0) \perp_q \dot{\gamma}_{qr}^*(0). \quad (41)$$

- Now, let us prove the Pythagorean identity when $\gamma_{pq} \perp_q \gamma_{qr}^*$. We use the Bregman 3-parameter identity [5] which generalizes the Euclidean law of cosines:

Property 1 (Bregman 3-parameter identity)

$$B_F(\theta_1 : \theta_2) = B_F(\theta_1 : \theta_3) + B_F(\theta_3 : \theta_2) - (\theta_1 - \theta_3)^\top (\nabla F(\theta_2) - \nabla F(\theta_3)) \geq 0 \quad (42)$$

Instantiating this identity with $\theta_1 = \theta(p)$, $\theta_2 = \theta(r)$ and $\theta_3 = \theta(q)$, and plugging the fact that $(\theta(p) - \theta(q))^\top (\nabla F(\theta(r)) - \nabla F(\theta(q))) = 0$, we get

$$B_F(\theta(p) : \theta(r)) = B_F(\theta(p) : \theta(q)) + B_F(\theta(q) : \theta(r)), \quad (43)$$

$$D_F(p : r) = D_F(p : q) + D_F(q : r). \quad (44)$$

□

Notice that the Bregman 3-parameter identity can be proved by checking that the left-hand side equals the right-hand side of Eq. 42. Another direct proof consists in writing:

$$B_F(\theta_1 : \theta_3) = F(\theta_1) - F(\theta_3) - (\theta_1 - \theta_3)^\top \nabla F(\theta_3), \quad (45)$$

$$B_F(\theta_3 : \theta_2) = F(\theta_3) - F(\theta_2) - (\theta_3 - \theta_2)^\top \nabla F(\theta_2), \quad (46)$$

$$B_F(\theta_1 : \theta_2) = F(\theta_1) - F(\theta_2) - (\theta_1 - \theta_2)^\top \nabla F(\theta_2). \quad (47)$$

Adding Eq. 46 with Eq. 47 and subtracting Eq. 45 from them, we get:

$$B_F(\theta_1 : \theta_3) + B_F(\theta_3 : \theta_2) - B_F(\theta_1 : \theta_2) = (\theta_1 - \theta_3)^\top (\nabla F(\theta_2) - \nabla F(\theta_3)), \quad (48)$$

from which it follows that

$$B_F(\theta_1 : \theta_2) = B_F(\theta_1 : \theta_3) + B_F(\theta_3 : \theta_2) - (\theta_1 - \theta_3)^\top (\nabla F(\theta_2) - \nabla F(\theta_3)). \quad (49)$$

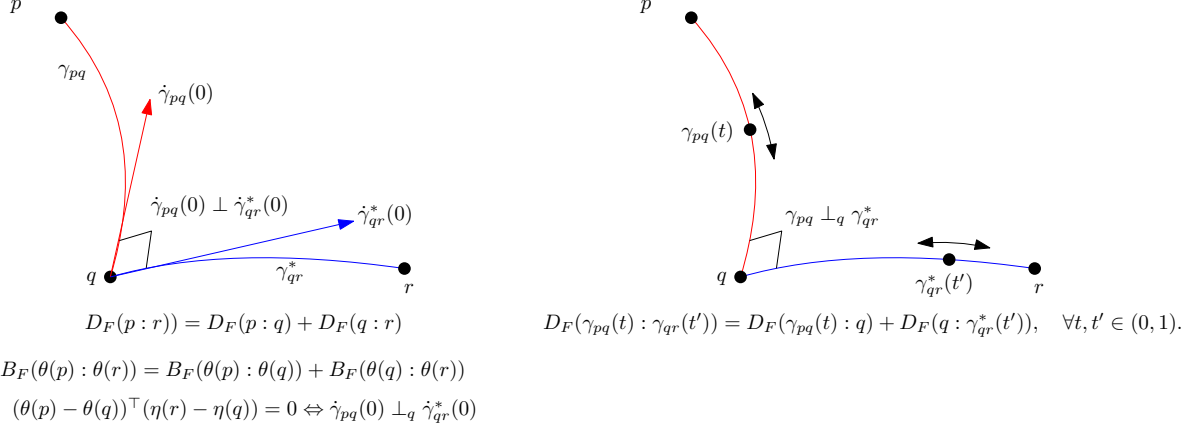


Figure 7: The generalized Pythagorean theorem in a dually flat space. Left: ordinary statement for dual-type geodesics γ_{pq} and γ_{qr}^* orthogonal at a point q . Right: Extended statement where the points can move along the dual geodesics $\gamma_{pq}(t)$ and $\gamma_{qr}^*(t')$.

More generally, we have

$$D_F(\gamma_{pq}(t) : q) + D_F(q : \gamma_{qr}^*(t')) = D_F(\gamma_{pq}(t) : \gamma_{qr}^*(t')), \quad \forall t, t' \in (0, 1). \quad (50)$$

That is, once we have a triple of points (p, q, r) for which the generalized Pythagorean theorem holds, we can build an infinite number of such triple of points: $(\gamma_{pq}(t), q, \gamma_{qr}^*(t'))$ for $t, t' \in (0, 1)$. Figure 7 illustrates this view of the generalized Pythagorean theorem.

Euclidean geometry with its ordinary Pythagoras' theorem is recovered as the special case of a self-dual Bregman manifold (when the dual potential functions coincide) induced by the Bregman generator $F_{\text{Euc}}(\theta) = \frac{1}{2}\theta^\top\theta$.

Notice that the tangent vector $v_{pq}^* = \dot{\gamma}_{pq}^*(0)$ of the dual geodesic $\gamma_{pq}^*(t)$ is written using the covariant components in the reciprocal basis of T_p as $\eta(q) - \eta(p)$. This tangent vector can be written equivalently using the contravariant coordinates as $\nabla^2 F^*(\eta(p)) \times [\eta(q) - \eta(p)]$. That is, $[v_{pq_i}^*] = \eta(q) - \eta(p)$ and $[v_{pq}^{*i}] = \nabla^2 F^*(\eta(p)) \times [\eta(q) - \eta(p)]$. Similarly, the tangent vector $v_{pq} = \dot{\gamma}_{pq}(0)$ of the primal geodesic $\gamma_{pq}(t)$ is written using the contravariant components in the basis of T_p as $\theta(q) - \theta(p)$. The covariant coordinates of this vector is $\nabla^2 F(\theta(p)) \times [\theta(q) - \theta(p)]$: $[v_{pq}^i] = \theta(q) - \theta(p)$ and $[v_{pq_i}] = \nabla^2 F(\theta(p)) \times [\theta(q) - \theta(p)]$. Figure 8 displays an example of two primal and dual geodesic arcs linking p to q with the tangent vectors $\dot{\gamma}_{pq}^*(0)$ at p of the dual geodesic γ_{pq} .

When we exchange the role played by points p and r in the above Pythagorean theorem, we obtain the following *dual* Pythagorean theorem:

Theorem 2 (Dual Pythagorean theorem) *When a dual geodesic γ_{pq}^* is orthogonal to a primal geodesic γ_{qr} at point q ($\dot{\gamma}_{pq}^* \perp_q \dot{\gamma}_{qr}$), we have $(\eta(p) - \eta(q))^\top (\theta(r) - \theta(q)) = 0$ and the following divergence identity:*

$$D_F^*(p : q) + D_F^*(q : r) = D_F^*(p : r), \quad (51)$$

or equivalently

$$D_F(r : q) + D_F(q : p) = D_F(r : p). \quad (52)$$

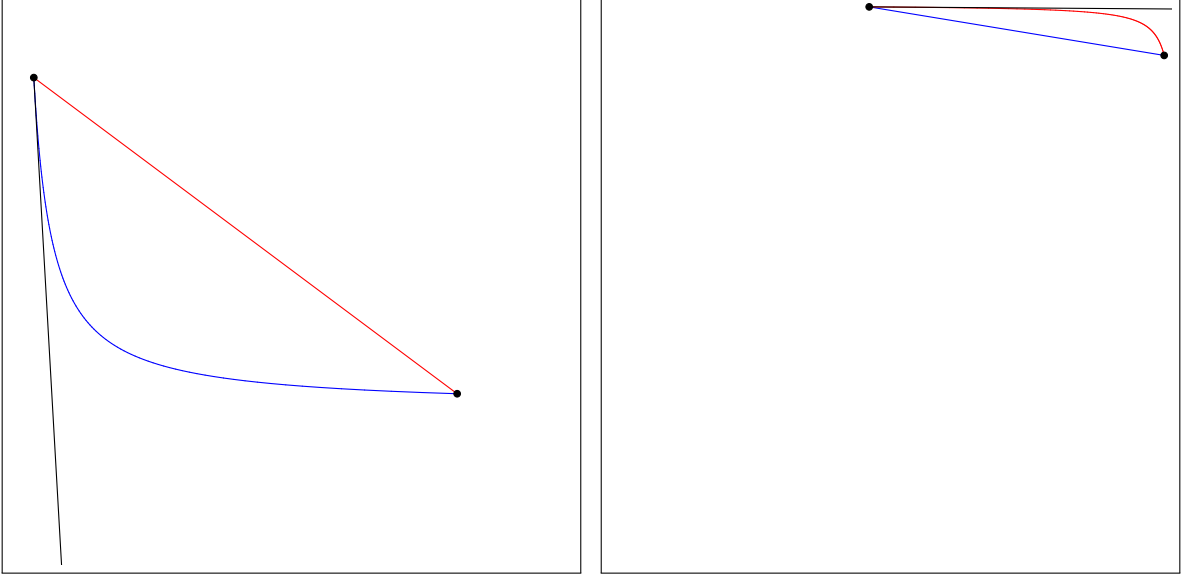


Figure 8: Two points p and q and their primal and dual geodesics visualized using the θ -coordinates (left) and the η -coordinates (right). The tangent vector $v_{pq}^* \in T_p$ to γ_{pq}^* is visualized in the θ -coordinates (left, black line segment), and the tangent vector $v_{pq} \in T_p$ to γ_{pq} is visualized in the η -coordinates (right, black line segment). Here, we considered the Itakura-Saito manifold with $\theta(p) = (0.17823054175936948, 1.746348492830485)$ and $\theta(q) = (1.6105239241969733, 0.6712015045558234)$.

Notice that we can write the Bregman generalized law of cosines of Eq. 42 geometrically (i.e., without relying on any prescribed coordinate system) as follows:

$$D_F(p : q) = D_F(p : r) + D_F(r : q) - g_r(\dot{\gamma}_{rp}(0), \dot{\gamma}_{rq}^*(0)) \geq 0, \quad (53)$$

$$= D_F(p : r) + D_F(r : q) - \|\dot{\gamma}_{rp}(0)\|_r \|\dot{\gamma}_{rq}^*(0)\|_r \cos(\alpha_r(\dot{\gamma}_{rp}, \dot{\gamma}_{rq}^*)). \quad (54)$$

It follows that

- when $\alpha_r(\dot{\gamma}_{rp}, \dot{\gamma}_{rq}^*) \in [0, \frac{\pi}{2})$ (acute angle), we have $D_F(p : q) < D_F(p : r) + D_F(r : q)$,
- when $\alpha_r(\dot{\gamma}_{rp}, \dot{\gamma}_{rq}^*) = \frac{\pi}{2}$ (right angle), we have $D_F(p : q) = D_F(p : r) + D_F(r : q)$, and
- when $\alpha_r(\dot{\gamma}_{rp}, \dot{\gamma}_{rq}^*) \in (\frac{\pi}{2}, \pi)$ (obtuse angle), we have $D_F(p : q) > D_F(p : r) + D_F(r : q)$.

Notice that when $F(\theta) = F_{\text{Euc}}(\theta) = \frac{1}{2}\theta^\top\theta$ (Euclidean geometry) and $\theta(r) = 0$, we get

$$\frac{1}{2}\|p - q\|^2 = \frac{1}{2}\|p\|^2 + \frac{1}{2}\|q\|^2 - \|p\|\|q\| \cos \alpha_r(p, q). \quad (55)$$

Multiplying by two both sides of Eq. 55, we recover the usual law of cosines of Euclidean geometry illustrated in Figure 9 with $a = \|p\|$, $b = \|q\|$, $c = \|p - q\|$, and $C = \alpha_r([rp], [rq])$:

$$c^2 = a^2 + b^2 - 2ab \cos C. \quad (56)$$

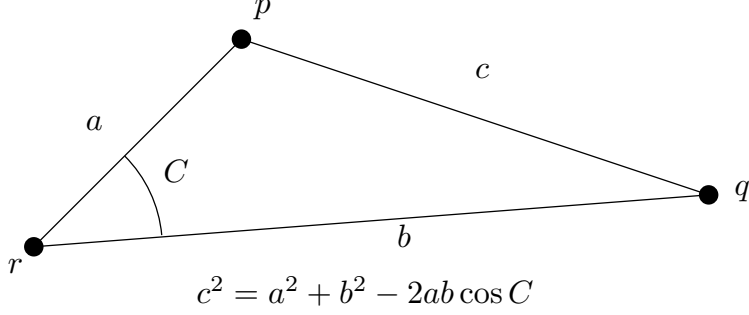


Figure 9: The Euclidean law of cosines.

We also have the following identity illustrated in Figure 10:

$$B_F(\theta_1 : \theta) + B_F(\theta_2 : \theta) = B_F\left(\theta_1 : \frac{\theta_1 + \theta_2}{2}\right) + B_F\left(\theta_2 : \frac{\theta_1 + \theta_2}{2}\right) + 2B_F\left(\frac{\theta_1 + \theta_2}{2} : \theta\right), \quad (57)$$

$$B_F(\theta_1 : \theta) + B_F(\theta_2 : \theta) = 2JB_F(\theta_1, \theta_2) + 2B_F\left(\frac{\theta_1 + \theta_2}{2} : \theta\right), \quad (58)$$

$$B_F(\theta_1 : \theta) + B_F(\theta_2 : \theta) = 2J_F(\theta_1, \theta_2) + 2B_F\left(\frac{\theta_1 + \theta_2}{2} : \theta\right), \quad (59)$$

where JB_F and J_F denote the *Jensen-Bregman divergence* [28] and the *Jensen divergence* [23], respectively:

$$JB_F(\theta_1, \theta_2) := \frac{1}{2} \left(B_F\left(\theta_1 : \frac{\theta_1 + \theta_2}{2}\right) + B_F\left(\theta_2 : \frac{\theta_1 + \theta_2}{2}\right) \right), \quad (60)$$

$$= \frac{F(\theta_1) + F(\theta_2)}{2} - F\left(\frac{\theta_1 + \theta_2}{2}\right) =: J_F(\theta_1, \theta_2). \quad (61)$$

The family of categorical distributions forms a mixture family [29] in information geometry for the Shannon negentropy generator F_{Shannon} , and we have $B_{F_{\text{Shannon}}}(\theta_1 : \theta_2) = \text{KL}(p_{\theta_1} : p_{\theta_2})$. It follows that for any three categorical distributions p , q , and r , we have

$$\text{KL}(p : r) + \text{KL}(q : r) = 2\text{JS}(p, q) + 2\text{KL}\left(\frac{p+q}{2} : r\right), \quad (62)$$

since $\frac{p+q}{2}$ is a categorical distribution. In general, the identity does not hold for members of an exponential family (i.e., Gaussian family) since the mixture density $\frac{p+q}{2}$ does not belong to the exponential family. The categorical family is a very special case of family that is *both* an exponential family and a mixture family [3].

Since there exists a bijection between regular exponential families and regular Bregman divergences [5], we can state the parallelogram-type identity of Eq. 57 for parametric densities $\{p_\theta\}$ belonging to the same exponential family [24] (with cumulant function F) with respect to both the Kullback-Leibler divergence and the *Bhattacharyya divergence* [23]

$$\text{Bhat}(p, q) := -\log \int \sqrt{p(x)q(x)} d\mu(x), \quad (63)$$

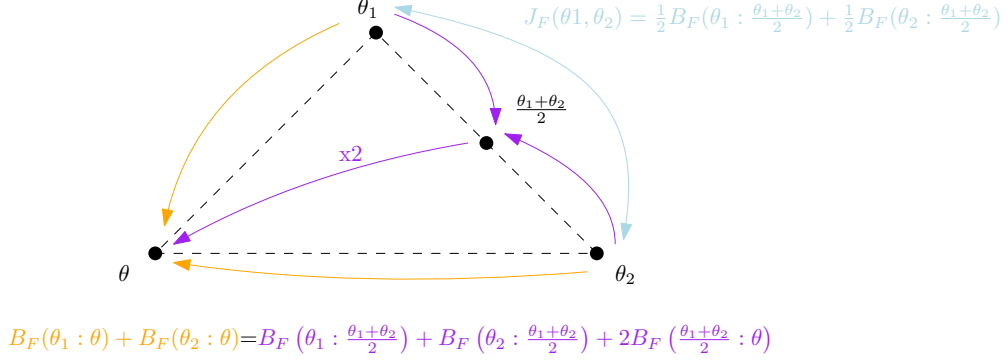


Figure 10: A parallelogram-type identity for Bregman divergences.

as:

$$\text{KL}(p_\theta : p_{\theta_1}) + \text{KL}(p_\theta : p_{\theta_2}) = 2\text{Bhat}(p_{\theta_1}, p_{\theta_2}) + 2\text{KL}\left(p_{\frac{\theta_1+\theta_2}{2}} : p_\theta\right), \quad (64)$$

since $\text{KL}(p_\theta : p_{\theta'}) = B_F(\theta' : \theta)$ and $\text{Bhat}(p_\theta : p_{\theta'}) = J_F(\theta, \theta')$ for densities p_θ and $p_{\theta'}$ belonging to the same exponential family. For example, the identity of Eq. 64 applies to any two densities of the Gaussian family.

The 3-parameter property of Bregman divergences is a particular instance of the following 4-parameter property [11] (a quadrilateral relation):

Property 2 (Bregman 4-parameter property) *For any four points p_1, p_2, q_1, q_2 , we have the following identity:*

$$\begin{aligned} B_F(\theta(p_1) : \theta(q_1)) + B_F(\theta(p_2) : \theta(q_2)) &= B_F(\theta(p_1) : \theta(q_2)) + B_F(\theta(p_2) : \theta(q_1)) \\ &\quad - (\theta(p_2) - \theta(p_1))^\top (\eta(q_1) - \eta(q_2)) = 0. \end{aligned} \quad (65)$$

Indeed, let $q_1 = p_1$. Then we recover:

$$\begin{aligned} B_F(\theta(p_2) : \theta(q_2)) &= B_F(\theta(p_1) : \theta(q_2)) + B_F(\theta(p_2) : \theta(q_1)) - (\theta(p_2) - \theta(p_1))^\top (\eta(q_2) - \eta(p_1)) \\ D_F(p_2 : q_2) &= D_F(p_2 : p_1) + D_F(p_1 : q_2) - g_{p_1}(\dot{\gamma}_{p_1 p_2}^*(0), \dot{\gamma}_{p_1 q_2}^*(0)). \end{aligned} \quad (66)$$

Similarly, let $q_2 = p_2$. Then we get:

$$\begin{aligned} B_F(\theta(p_1) : \theta(q_1)) &= B_F(\theta(p_1) : \theta(p_2)) + B_F(\theta(p_2) : \theta(q_1)) - (\theta(p_1) - \theta(p_2))^\top (\eta(q_1) - \eta(p_2)) \\ D_F(p_1 : q_1) &= D_F(p_1 : p_2) + D_F(p_2 : q_1) - g_{p_2}(\dot{\gamma}_{p_2 p_1}^*(0), \dot{\gamma}_{p_2 q_1}^*(0)). \end{aligned} \quad (68)$$

To derive the 4-parameter identity, we use twice the 3-parameter identity as follows:

$$B_F(\theta_1 : \theta_3) = B_F(\theta_1 : \theta_2) + B_F(\theta_2 : \theta_3) - (\theta_3 - \theta_2)^\top (\nabla F(\theta_1) - \nabla F(\theta_2)), \quad (70)$$

$$B_F(\theta_4 : \theta_3) = B_F(\theta_4 : \theta_2) + B_F(\theta_2 : \theta_3) - (\theta_3 - \theta_2)^\top (\nabla F(\theta_4) - \nabla F(\theta_2)). \quad (71)$$

Indeed, subtracting Eq. 71 from Eq. 70, we get

$$B_F(\theta_1 : \theta_3) - B_F(\theta_4 : \theta_3) = B_F(\theta_1 : \theta_2) - B_F(\theta_4 : \theta_2) - (\theta_3 - \theta_2)^\top (\nabla F(\theta_1) - \nabla F(\theta_4)). \quad (72)$$

We can interpret geometrically the 4-parameter identity as follows:

$$D_F(p_1 : p_3) - D_F(p_4 : p_3) = D_F(p_1 : p_2) - D_F(p_4 : p_2) - g_{p_2}(\dot{\gamma}_{p_2 p_3}(0), \dot{\gamma}_{p_2 p_1}^*(0)) + g_{p_2}(\dot{\gamma}_{p_2 p_3}(0), \dot{\gamma}_{p_2 p_4}^*(0)). \quad (73)$$

Note that the Bregman 4-parameter identity is said parallelogram-type, because if we choose $F_{\text{Euc}}(\theta) = \frac{1}{2}\theta^\top\theta = \frac{1}{2}\|\theta\|_2^2$, then we have $B_{F_{\text{Euc}}}(\theta : \theta') = \frac{1}{2}\|\theta - \theta'\|_2^2$, and the 4-parameter identity becomes for $\theta = 0$:

$$\frac{1}{2}\|\theta_1\|_2^2 + \frac{1}{2}\|\theta_2\|_2^2 = \left\| \frac{\theta_1 - \theta_2}{2} \right\|_2^2 + \left\| \frac{\theta_1 + \theta_2}{2} \right\|_2^2, \quad (74)$$

$$2\|\theta_1\|_2^2 + 2\|\theta_2\|_2^2 = \|\theta_1 - \theta_2\|_2^2 + \|\theta_1 + \theta_2\|_2^2, \quad (75)$$

the usual parallelogram identity for the L_2 -normed space.

Finally, let us mention some special submanifolds in dually flat spaces: A k -dimensional submanifold $S \subset M$ of a dually flat manifold M is said ∇ -autoparallel [3] (∇^* -autoparallel) iff. the sets of points of S can be described by a k -dimensional affine flat in the θ -coordinate system (η -coordinate system, respectively). Primal γ_{pq} geodesics are 1D ∇ -autoparallel submanifolds and dual γ_{pq}^* geodesics are 1D ∇^* -autoparallel submanifolds. Notice that the intersection of θ -flats is a θ -flat, but the intersection of a θ -flat with a η -flat is in general neither a θ -flat nor a η -flat.

In a Bregman manifold, we can also express the divergence between two points p and q using the *Fenchel-Young divergence* A_F (also called the canonical divergence of dually flat spaces):

$$D_F(p : q) = A_F(\theta(p) : \eta(q)) := F((\theta(p)) + F^*(\eta(q)) - \theta(p)^\top \eta(q). \quad (76)$$

Thus we have

$$D_F(p : q) = B_F(\theta(p) : \theta(q)) = A_F(\theta(p) : \eta(q)) = A_{F^*}(\eta(q) : \theta(p)) = B_{F^*}(\eta(q) : \eta(p)) = D_{F^*}(q : p), \quad (77)$$

and $D_{F^*}(q : p) = D_{F^*}(q : p) = D_F(p : q)$ (where D_{F^*} is the reverse divergence).

2.4 Some examples of Bregman manifolds

We describe concisely the Mahalanobis manifolds in §2.4.1, the extended Kullback-Leibler manifold in §2.4.2, the Itakura-Saito manifold in §2.4.3, and the multinoulli manifolds (§2.4.4).

2.4.1 The Mahalanobis manifolds

Consider the case where the Bregman generator is defined by

$$F_Q(\theta) = \frac{1}{2}\theta^\top Q\theta, \quad (78)$$

for a prescribed symmetric positive-definite $D \times D$ matrix $Q \succ 0$. The Legendre-Fenchel convex conjugate [18, 19] is

$$F^*(\eta) = \frac{1}{2}\eta^\top Q^{-1}\eta = F_{Q^{-1}}(\eta), \quad (79)$$

and it follows that

$$\eta(\theta) = \nabla F_Q(\theta) = Q\theta, \quad \theta(\eta) = \nabla F_Q^*(\eta) = Q^{-1}\eta. \quad (80)$$

The dual Riemannian metrics are

$$[g_{ij}] = \nabla^2 F_Q(\theta) = Q, \quad (81)$$

$$[g^{*ij}] = \nabla^2 F_Q^*(\eta) = Q^{-1}. \quad (82)$$

The dual geodesics γ_{pq} and γ_{qp}^* in a Mahalanobis manifold coincide. The dual Bregman divergences are squared Mahalanobis distances [17, 26]:

$$B_{F_Q}(\theta_1 : \theta_2) = \frac{1}{2}(\theta_1 - \theta_2)^\top Q(\theta_1 - \theta_2), \quad (83)$$

and

$$B_{F_Q^*}(\eta_1 : \eta_2) = \frac{1}{2}(\eta_1 - \eta_2)^\top Q^{-1}(\eta_1 - \eta_2). \quad (84)$$

We check that

$$B_{F_Q^*}(\eta_2 : \eta_1) = \frac{1}{2}(Q(\theta_2 - \theta_1))^\top Q^{-1}Q(\theta_2 - \theta_1) = B_{F_Q}(\theta_1 : \theta_2), \quad (85)$$

since $Q^\top = Q$. The squared Mahalanobis Bregman divergences are provably the only symmetric Bregman divergences [6]. In particular, when $Q = I$, the identity matrix, the dual Bregman divergences B_F and B_F^* coincide with half of the squared Euclidean distance $D_E(\theta_1, \theta_2) = \frac{1}{2}(\theta_2 - \theta_1)^\top(\theta_2 - \theta_1)$. By using the Cholesky decomposition of Q , i.e., $Q = LL^\top$ where L is a lower triangular matrix with positive diagonal entries, we have $B_{F_Q}(\theta_1 : \theta_2) = B_{F_I}(L^\top\theta_1 : L^\top\theta_2) = \|L^\top(\theta_1 - \theta_2)\|^2$, where I denotes the identity matrix. Notice that the squared Mahalanobis divergences B_{F_Q} are non-separable Bregman divergences whenever Q has non-zero off-diagonal elements.

2.4.2 The Kullback-Leibler manifold

The extended Shannon negative entropy [23]

$$F_{\text{KL}}(\theta) = \sum_{i=1}^D \theta^i \log \theta^i - \theta^i \quad (86)$$

is a strictly convex and C^3 function on $\Theta = \mathbb{R}_{++}^D$, i.e., a separable Bregman generator. Here, we consider the positive orthant domain instead of the probability simplex hence the name extended Shannon negentropy. We have the following conversion formula between the primal and dual coordinates:

$$\eta(\theta) = \nabla F_{\text{KL}}(\theta) = [\log \theta^i], \quad \theta(\eta) = \nabla F_{\text{KL}}^*(\eta) = [\exp \eta^i]. \quad (87)$$

The Legendre convex conjugate is

$$F_{\text{KL}}^*(\eta) = \theta(\eta)^\top \eta - F(\theta(\eta)) = \sum_{i=1}^D \exp(\eta^i). \quad (88)$$

The dual Riemannian metrics are

$$[g_{ij}] = \nabla^2 F_{\text{KL}}(\theta) = \text{diag} \left(\frac{1}{\theta^1}, \dots, \frac{1}{\theta^D} \right), \quad [g^{*ij}] = \nabla^2 F_{\text{KL}}^*(\eta) = \text{diag} (\exp(\eta^1), \dots, \exp(\eta^D)). \quad (89)$$

The dual Bregman divergences are

$$B_{F_{\text{KL}}}(\theta_1 : \theta_2) = \sum_{i=1}^D \theta_1^i \log \frac{\theta_1^i}{\theta_2^i} + \theta_2^i - \theta_1^i, \quad (90)$$

$$B_{F_{\text{KL}}^*}(\eta_1 : \eta_2) = \sum_{i=1}^D \exp(\eta_1^i) - \exp(\eta_2^i) - (\eta_1^i - \eta_2^i) \exp(\eta_2^i) = B_{F_{\text{KL}}}(\theta(\eta_2) : \theta(\eta_1)). \quad (91)$$

2.4.3 Itakura-Saito manifold

The D -dimensional Burg information (i.e., Burg negative entropy [27, 23]) is defined by the following separable convex generator:

$$F_{\text{IS}}(\theta) = - \sum_{i=1}^D \log(\theta^i). \quad (92)$$

We have

$$\eta(\theta) = \nabla F(\theta) = \left[-\frac{1}{\theta^i} \right]_i, \quad (93)$$

and the Bregman divergence is called the Itakura-Saito divergence [6]:

$$B_{F_{\text{IS}}}(\theta_1 : \theta_2) = \sum_{i=1}^D \frac{\theta_1^i}{\theta_2^i} - \log \frac{\theta_1^i}{\theta_2^i} - 1. \quad (94)$$

We convex η -coordinates to θ -coordinates as follows:

$$\theta(\eta) = \left[-\frac{1}{\eta^i} \right]_i, \quad (95)$$

and the dual Bregman generator is

$$F_{\text{IS}}^*(\eta) = \eta^\top \theta(\eta) - F_{\text{IS}}(\theta(\eta)) = -D + \sum_{i=1}^D \log \left(-\frac{1}{\eta^i} \right) = -D - \sum_{i=1}^D \log(-\eta_i), \quad (96)$$

where $\eta \in \mathbb{R}_{--}^D$. The dual Bregman divergence is

$$B_{F_{\text{IS}}^*}(\eta_1 : \eta_2) = \sum_{i=1}^D \frac{\eta_1^i}{\eta_2^i} - \log \frac{\eta_1^i}{\eta_2^i} - 1. \quad (97)$$

We check that

$$B_{F_{\text{IS}}^*}(\eta_2 : \eta_1) = B_{F_{\text{IS}}}(\theta_1 : \theta_2). \quad (98)$$

The dual Riemannian metric tensors are

$$[g_{ij}] = \nabla^2 F_{\text{IS}}(\theta) = \text{diag} \left(\frac{1}{\text{sqr}(\theta^1)}, \dots, \frac{1}{\text{sqr}(\theta^D)} \right), \quad [g^{*ij}] = \nabla^2 F_{\text{IS}}^*(\eta) = \text{diag} \left(\frac{1}{\text{sqr}(\eta^1)}, \dots, \frac{1}{\text{sqr}(\eta^D)} \right). \quad (99)$$

2.4.4 The multinoulli manifolds

We can build a dually flat space from any strictly convex and C^3 convex function F [20] which also defines a Bregman generator. In particular, we can use the *log-normalizer* (also called cumulant function or log-partition function) of a regular exponential family [5] as such a Bregman generator [25]. Let us consider the multinoulli family (i.e., the multinomial family for a single trial also called the family of categorical distributions). The probability of a multinoulli distribution with d categories c_1, \dots, c_d such that $\Pr(x = c_i) = \lambda_i$ is:

$$\Pr(x) = \lambda_1^{x_1} \times \dots \times \lambda_d^{x_d}, \quad (100)$$

with $x_i \in \{0, 1\}$ and $\sum_{i=1}^d x_i = 1$. Let us write the multinoulli probability mass function in the canonical form of an exponential family as

$$\lambda_1^{x_1} \times \dots \times \lambda_d^{x_d} = \exp\left(\sum_{i=1}^d x_i \log \lambda_i\right), \quad (101)$$

$$= \exp\left(\sum_{i=1}^{d-1} x_i \log \lambda_i + \underbrace{\left(1 - \sum_{i=1}^{d-1} x_i\right)}_{x_d} \log \lambda_d\right), \quad (102)$$

$$= \exp\left(\sum_{i=1}^{d-1} x_i \theta_i - F(\theta)\right), \quad (103)$$

$$(104)$$

with the natural parameter $\theta_i = \log \frac{\lambda_i}{\lambda_d}$ for $i \in \{1, \dots, d-1\}$. The multinoulli distribution is an exponential family of order $D = d-1$. The natural parameter space Θ is $\mathbb{R}^D = \mathbb{R}^{d-1}$. We can convert back the natural parameter θ to the original parameters λ as follows:

$$\lambda(\theta) = \begin{cases} \lambda_i = \frac{\exp(\theta_i)}{1 + \sum_{i=1}^D \exp(\theta_i)}, & \text{for } i \in \{1, \dots, D\} \\ \lambda_d = \frac{1}{1 + \sum_{i=1}^D \exp(\theta_i)}. \end{cases} \quad (105)$$

The log-normalizer is

$$F_{\text{Mult}}(\theta) = -\log \lambda_d = \log \left(1 + \sum_{i=1}^D \exp(\theta_i)\right). \quad (106)$$

The gradient of the log-normalizer is

$$\eta(\theta) = \nabla F_{\text{Mult}}(\theta) = \left[\frac{\exp(\theta_i)}{1 + \sum_{i=1}^D \exp(\theta_i)} \right]_i, \quad (107)$$

and the reciprocal gradient is

$$\theta(\eta) = \nabla G_{\text{Mult}}(\eta) = \left[\log \frac{\eta_i}{1 - \sum_{i=1}^D \eta_i} \right]_i. \quad (108)$$

The convex conjugate of F is

$$G_{\text{Mult}}(\eta) = \eta^\top \theta(\eta) - F(\theta(\eta)) = \sum_i \eta_i \log \eta_i + \left(1 - \sum_i \eta_i\right) \log \left(1 - \sum_i \eta_i\right). \quad (109)$$

It follows that the Riemannian metric and dual Riemannian metric are Hessians of the potential functions $F_{\text{Mult}}(\theta)$ and $G_{\text{Mult}}(\eta)$, respectively:

$$[\nabla^2 F_{\text{Mult}}(\theta)]_{ij} = \begin{cases} -\frac{\exp(\theta_i + \theta_j)}{(1 + \sum_i \exp(\theta_i))^2} & \text{if } i \neq j, \\ \frac{\exp(\theta_i)}{(1 + \sum_i \exp(\theta_i))} - \frac{\exp(2\theta_i)}{(1 + \sum_i \exp(\theta_i))^2} & \text{if } i = j \end{cases} \quad (110)$$

$$\nabla^2 G_{\text{Mult}}(\eta) = \frac{1}{1 - \sum_i \eta_i} \mathbf{1}_M + \text{diag} \left(\frac{1}{\eta_1}, \dots, \frac{1}{\eta_D} \right) = \begin{cases} \frac{1}{1 - \sum_i \eta_i} & \text{if } i \neq j, \\ \frac{1}{1 - \sum_i \eta_i} + \frac{1}{\eta_i} & \text{if } i = j \end{cases}, \quad (111)$$

where $\mathbf{1}_M$ denotes the $D \times D$ -matrix with all entries equal to 1, and $\text{diag}(x_1, \dots, x_D)$ the diagonal matrix with diagonal elements x_1, \dots, x_D .

The dual Bregman divergences are

$$B_{F_{\text{Mult}}}(\theta_1 : \theta_2) = \text{KL}^*(p_{\lambda(\theta_1)} : p_{\lambda(\theta_2)}) = \text{KL}(p_{\lambda(\theta_2)} : p_{\lambda(\theta_1)}), \quad (112)$$

$$B_{G_{\text{Mult}}}(\eta_1 : \eta_2) = \text{KL}(p_{\lambda(\eta_1)} : p_{\lambda(\eta_2)}), \quad (113)$$

$$(114)$$

where KL is the discrete Kullback-Leibler divergence and KL^* the reverse Kullback-Leibler divergence. We convert the expectation parameter η to the original parameter λ as follows:

$$\lambda(\eta) = \begin{cases} \lambda_i = \eta_i, & \text{for } i \in \{1, \dots, D\} \\ \lambda_d = 1 - \sum_{i=1}^D \eta_i. \end{cases} \quad (115)$$

In general, the Bregman divergence induced by log-normalizer of an exponential family amounts to a reverse Kullback-Leibler divergence [25]. Notice that the non-separable log-normalizer of a multinomial family yields a nice example of a non-separable Bregman divergence. The multinoulli manifold is called the *Bernoulli manifold* when $D = 1$ (i.e., $d = 2$), and the trinoulli manifold when $D = 2$ (i.e., $d = 3$).

2.5 Bregman balls and Bregman spheres

The space of Bregman spheres and Bregman balls was investigated in [6]. Here, we report the parametric equations of Bregman spheres which allow one to draw them. Let us consider a *separable* (Bregman) distance $D(\theta_1 : \theta_2)$ between two d -dimensional vectors $\theta_1 = (\theta_1^1, \dots, \theta_1^d)$ and $\theta_2 = (\theta_2^1, \dots, \theta_2^d)$:

$$D(\theta_1 : \theta_2) = \sum_{i=1}^d D_i(\theta_1^i : \theta_2^i),$$

where the $D_i(\cdot, \cdot)$'s denote the scalar distances. To avoid confusion with the distance D , the dimension of the spaces is denoted by d in this section. For example, we may consider the discrete f -divergences [10] which includes the Kullback-Leibler divergence, or the Bregman divergences [7]

which includes the extended Kullback-Leibler divergence and the Itakura-Saito divergence. The Kullback-Leibler divergence between two densities of an exponential family amounts to a Bregman divergence [4].

Let us define a D -sphere of center θ_c and radius $r \geq 0$ as follows:

$$\text{sphere}_D(\theta_c, r) := \{\theta : D(\theta_c : \theta) = r\}.$$

In practice, we can visualize a D -sphere by drawing the *implicit function* $f(\theta) := D(\theta_c : \theta) - r$. Plotting packages such as `gnuplot`⁶ use either a marching cube technique or a fast quadtree approximation algorithm to rasterize these implicit functions.

Here, we are concerned with reporting parametric equations of D -spheres for separable distances D . Let us characterize the coordinates θ^i of a point θ belonging to a D -sphere $\text{sphere}_D(\theta_c, r)$ as follows:

$$\begin{cases} D_1(\theta_c^1 : \theta^1) & = u_1 \geq 0, \\ \dots & \\ D_d(\theta_c^d : \theta^d) & = u_d \geq 0, \\ u_1 + \dots + u_d & = r \end{cases}$$

For f -divergences and Bregman divergences, the equation $D(c, x) = u$ for a scalar distance D admits two solutions $x_{D,c,u;1} \geq u$ and $x_{D,c,u;-1} \leq u$ for $r > 0$, where ± 1 denotes the sign to localize the interval endpoint with respect to the center c . It follows that the parametric equation of a d -dimensional D -sphere can be written independently on the 2^d orthants. For $o \in \{-1, 1\} \times \{-1, 1\} \subset \mathbb{R}^d$, let O_o denote the orthant

$$O_o = \{\theta : \theta^i \geq \text{sign}(o^i)\theta_c^i\}.$$

Then the equation of the D -sphere on the orthant O_o is

$$\left(x_{D_1, \theta_c^1, u_1; \text{sign}(o^1)(o)}, \dots, x_{D_d, \theta_c^d, u_d; \text{sign}(o^d)(o)} \right), \\ u_1 \in [0, r], u_2 \in [0, r - u_1], \dots, u_d \in \left[0, r - \sum_{i=1}^{d-2} u_i \right].$$

Thus if we know the parametric equations of a D -sphere on two opposite orthants, we can deduce the full parameteric equation of the D -sphere. Notices that all axis-parallel boxes

$$B = \prod_{i=1}^d [x_{D_i, \theta_c^i, u_i; -1}, x_{D_i, \theta_c^i, u_i; 1}]$$

are tangent at the D -sphere at its 2^d corners. Figure 11 illustrates this property for a 2D extended Kullback-Leibler circle (left) and a 2D Itakura-Saito circle (right).

We now illustrate how to get the parametric equations of relative entropic spheres defined with respect to the Kullback-Leibler divergence and the Itakura-Saito divergence in terms of the branches of the Lambert W function [8].

⁶<http://www.gnuplot.info/>

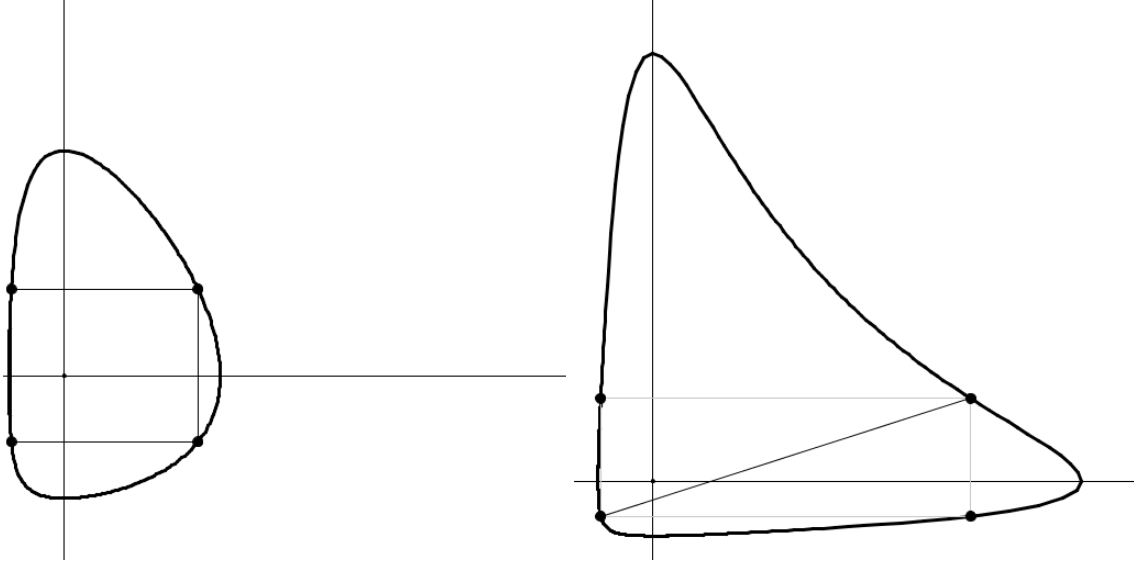


Figure 11: D -spheres with respect to separable distances shown with a random box tangent at its vertices: To plot a D -sphere, we only need to know the parametric equations on two opposite orthants to deduce the other orthants.

2.5.1 Parameterization of the Kullback-Leibler spheres

The scalar extended Kullback-Leibler divergence defined on \mathbb{R}^+ is defined by:

$$D_{\text{KL}}[\theta_c : \theta] := \theta_c \log \frac{\theta_c}{\theta} + \theta - \theta_c.$$

The two solutions of this equation will rely on two branches of the Lambert W function [8]. Indeed, the equation $xe^x = a$ solves as

$$x = \begin{cases} W_0(a) & \text{if } a \geq \frac{1}{e} \\ W_{-1}(a) & \text{if } -\frac{1}{e} \leq a < 0 \end{cases}$$

To solve $D_{\text{KL}}[\theta_c : \theta] = u$ for $\theta_c \in (0, 1)$ and $u \geq 0$ amounts to solve the equation

$$\begin{aligned} \theta_c \log \frac{\theta_c}{\theta} + \theta &= u + \theta_c, \\ \theta - \theta_c \log \theta &= u + \theta_c(1 - \log \theta_c). \end{aligned}$$

We get the two solutions using the two branches W_0 and W_{-1} of the Lambert W function [8]:

$$x_{D_{\text{KL}}, \theta_c, u; -1} = -\theta_c W_0 \left(-\exp \left(-\frac{u}{\theta_c} - 1 \right) \right), \quad (116)$$

$$x_{D_{\text{KL}}, \theta_c, u; 1} = -\theta_c W_{-1} \left(-\exp \left(-\frac{u}{\theta_c} - 1 \right) \right). \quad (117)$$

Figure 12 displays a D_{KL} sphere in two dimensions by plotting the four quadrant parameterizations. See the corresponding online video.⁷ The restriction of the KL sphere to the hyperplane

⁷<https://www.youtube.com/watch?v=pgDwWJ1DQFY>

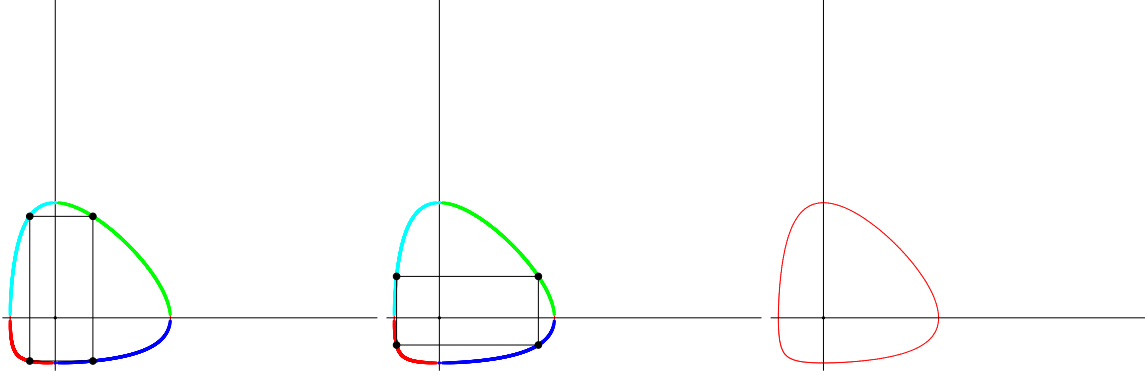


Figure 12: Plotting the parametric equations on each quadrant of an extended Kullback-Leibler circle sphere $_{D_{\text{KL}}}((\frac{1}{2}, \frac{1}{2}), \frac{1}{2})$ on the plane. The first two plots show some inscribed isorectangles tangent at its four vertices to the extended Kullback-Leibler circle.

$\sum_{i=1}^d \theta^i = 1$ yields a Kullback-Leibler sphere on the $(d - 1)$ -dimensional probability simplex (i.e., standard simplex) embedded in \mathbb{R}^d .

Figure 13 displays the four parameterized curves of the extended Kullback-Leibler circle.

2.6 Parameterization of the Itakura-Saito spheres

The scalar Itakura-Saito divergence defined on \mathbb{R}^+ is

$$D_{\text{IS}}[\theta_c : \theta] = \frac{\theta_c}{\theta} - \log \frac{\theta_c}{\theta} - 1.$$

The Itakura-Saito divergence is a Bregman divergence for the generator $F(x) = -\log u$, and can thus be interpreted as a relative entropy.

For the Itakura-Saito divergence, we have to solve the following equation:

$$\frac{\theta_c}{\theta} - \log \left(\frac{\theta_c}{\theta} \right) - 1 = u.$$

Since $\frac{\theta_c}{\theta} = \log \exp(\frac{\theta_c}{\theta})$, we get:

$$x_{D_{\text{IS}}, \theta_c, u; -1} = -\frac{c_x}{W_{-1}(-e^{-u-1})}, \quad (118)$$

$$x_{D_{\text{IS}}, \theta_c, u; 1} = -\frac{c_x}{W_0(-e^{-u-1})}. \quad (119)$$

Figure 14 displays a D_{IS} sphere in two dimensions by plotting the four quadrant parameterizations. See the corresponding online video.⁸

Figure 15 displays the four parameterized curves of the Itakura-Saito circle.

Figure 16 visualizes and compares the parametric equations on a quadrant of the extended Kullback-Leibler circle and the Itakura-Saito circle.

⁸<https://www.youtube.com/watch?v=b4eJu1TT-to>

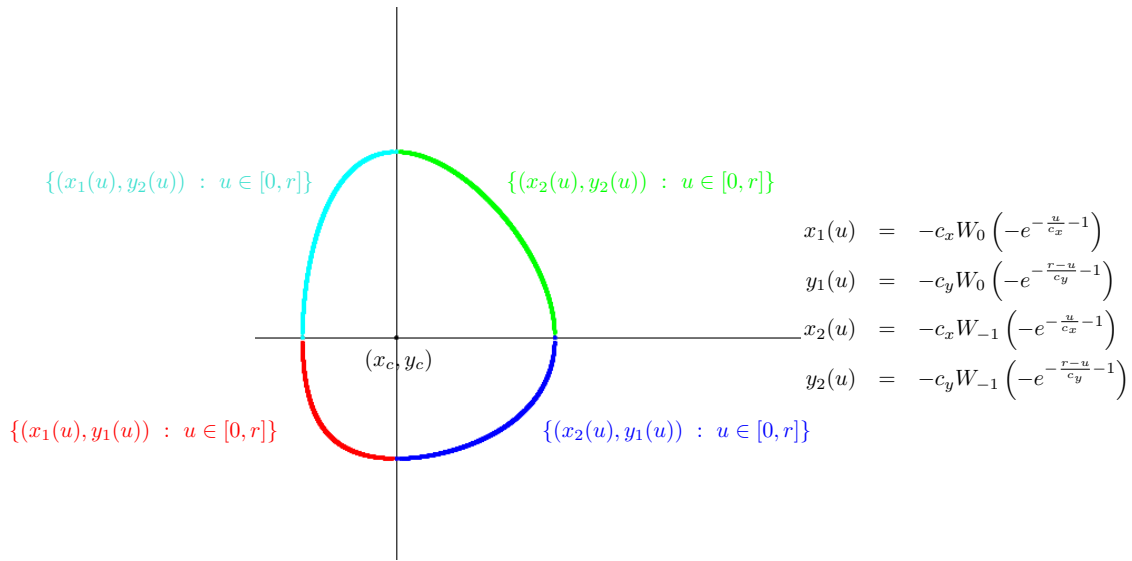


Figure 13: Quadrant-based parameterized curves of the extended Kullback-Leibler circle.

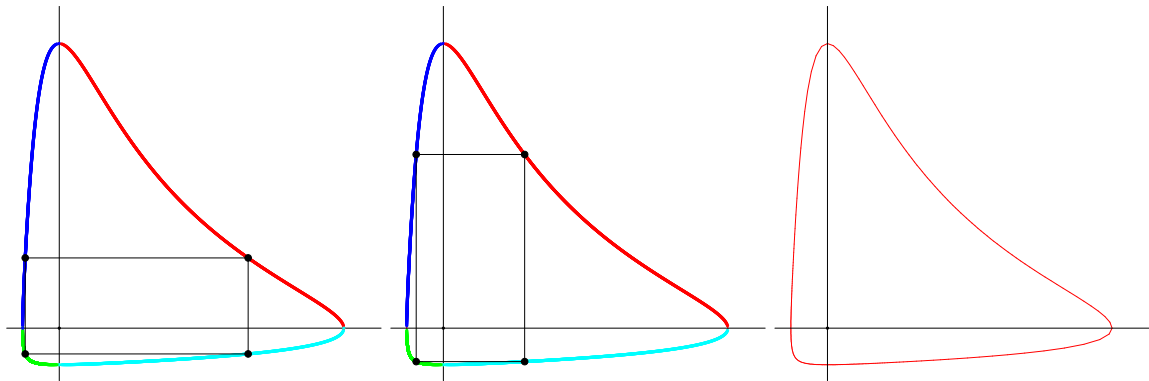


Figure 14: Plotting the parametric equations on each quadrant of a Itakura-Saito circle sphere $_{D_{\text{IS}}}((\frac{1}{2}, \frac{1}{2}), 1)$ on the plane. The first two plots show some inscribed isorectangles tangent at its four corners to the IS sphere.

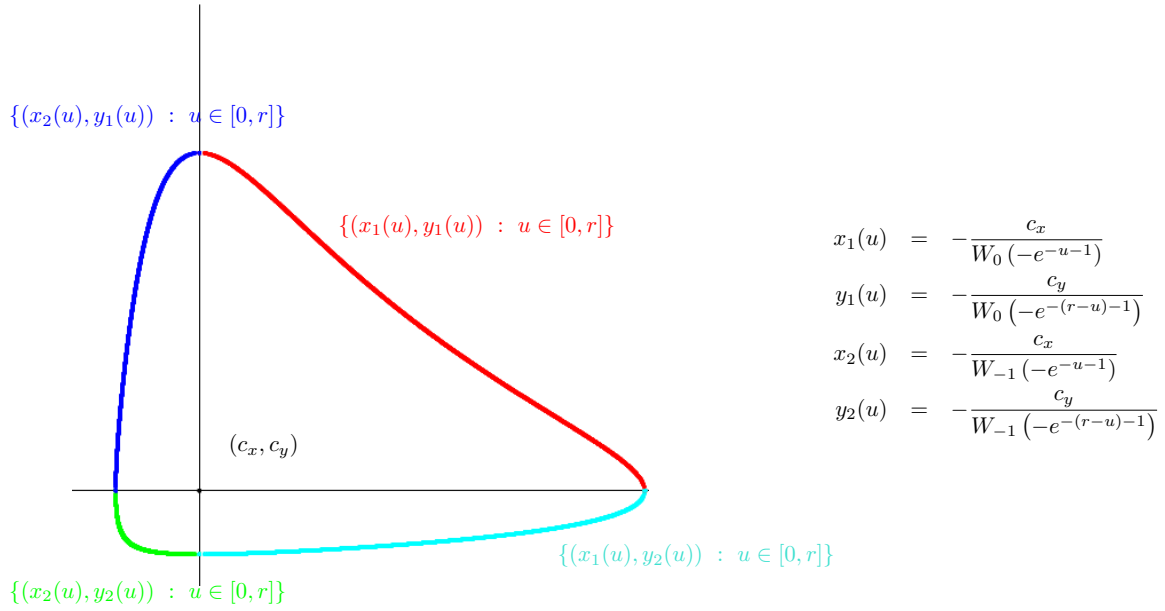


Figure 15: Quadrant-based parameterized curves of the extended Itakura-Saito circle.

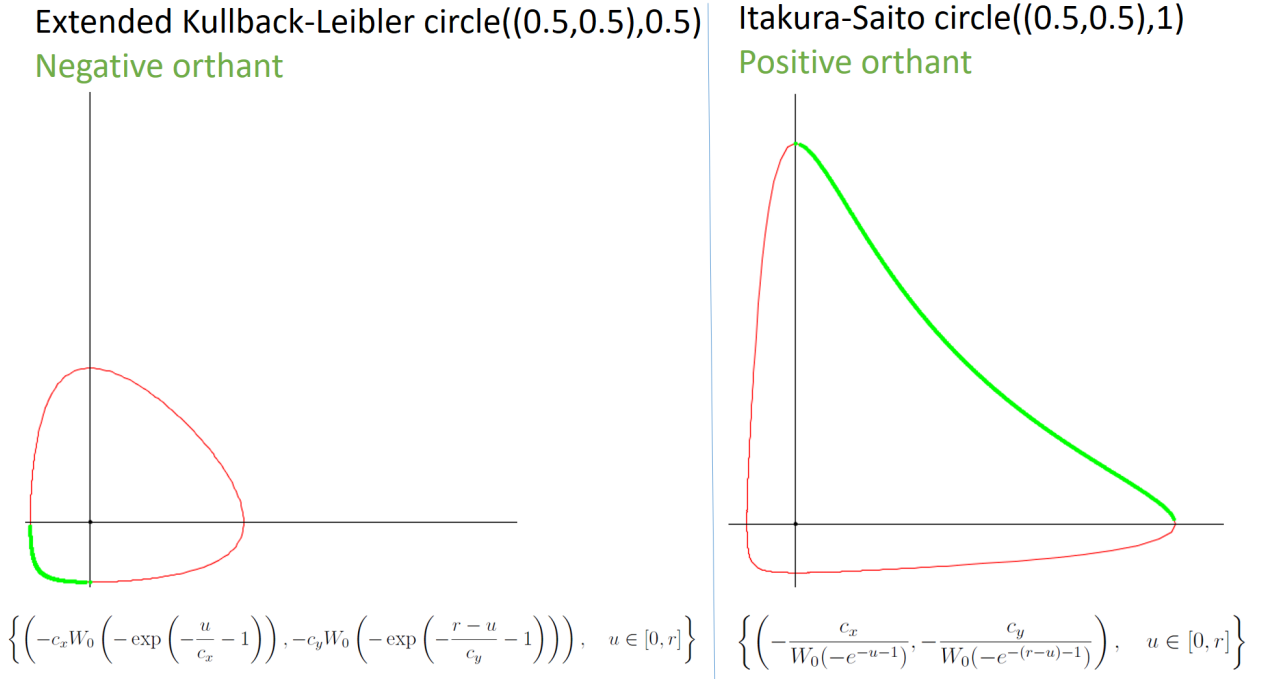


Figure 16: Parametric equations of the extended Kullback-Leibler circle and the Itakura-Saito circle on a quadrant (green part).

3 Geodesic ∇ -triangles with one, two, or three interior right angles

3.1 Geodesic ∇ -triangles with one interior right angle

To build a geodesic ∇ -triangle with a right angle, fix two points p and q (i.e., the first two triangle vertices), and consider the location of the third triangle vertex point r such that $\gamma_{qr} \perp_q \gamma_{qp}$ (i.e., $\dot{\gamma}_{qr}(0) \perp_q \dot{\gamma}_{qp}(0)$). We end up with the following linear equation which defines a θ -flat H_q^θ :

$$H_q^\theta : \theta_r^\top \nabla^2 F(\theta_q) \theta_{pq} = \theta_q^\top \nabla^2 F(\theta_q) \theta_{pq}. \quad (120)$$

By restricting the solution $r \in H_q^\theta$ to the manifold M , we get:

Proposition 1 *The locii of points r of a ∇ -triangle that form a right angle at q is $H_q^\theta \cap M$.*

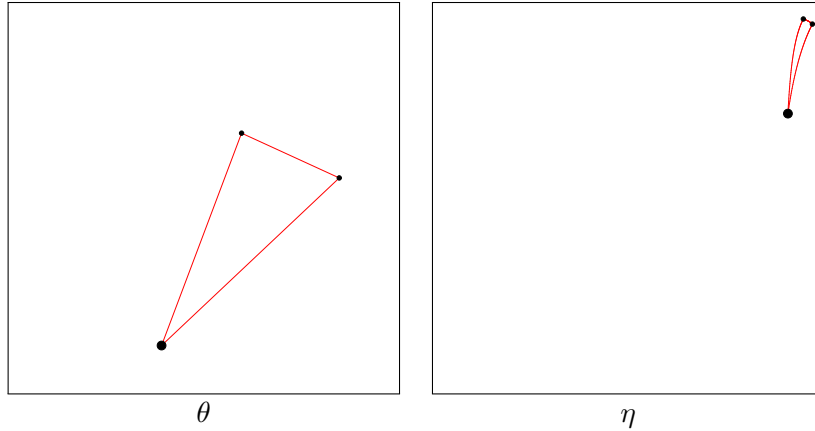


Figure 17: An example of a geodesic ∇ -triangle with a right angle at q : (thicker vertex is r).

Figure 17 displays that a ∇ -triangle with one right angle $\alpha_q(r, p) = \frac{\pi}{2}$ in the Itakura-Saito manifold: $\theta(p) = (1.2885253880864789, 3.4136709176658546)$,

$\theta(q) = (4.9336774965526065, 1.656631440605195)$,

$\theta(r) = (3.5399193730133236, 4.6263857851449846)$.

The interior angles of the ∇ -triangle are $\alpha_p(q, r) = 1.8276508176456936$,

$\alpha_q(p, r) = 1.5707963267948966$

and $\alpha_r(p, q) = 1.1542328404967954$.

That total sum of the interior angles are 4.552679984937385 radians (equivalent to about 260.8 degrees).

3.2 Geodesic ∇ -triangles with two interior right angles

We now report the construction of two right angle ∇ -triangles. That is, geodesic triangles with all primal geodesic edges (i.e., ∇ -triangle), with both the right angles $\alpha_p(q, r) = 90^\circ$ and $\alpha_q(p, r) = 90^\circ$. Figure 18 displays such a double right angle ∇ -triangle for the Burg negentropy generator $F_{\text{IS}}(\theta)$ yielding the Itakura-Saito divergence. Observe that because the metric tensor field g is not a scalar

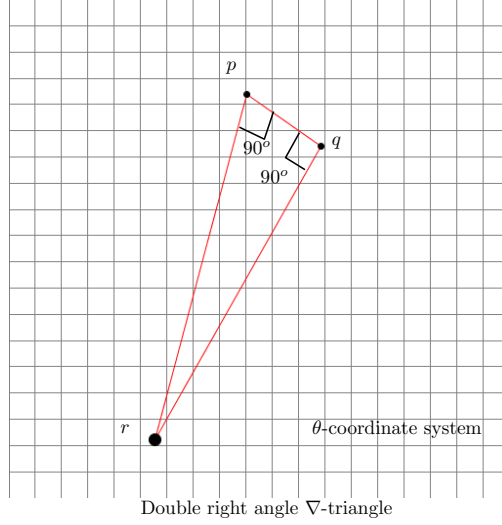


Figure 18: An example of double right angle ∇ -triangle visualized in the primal θ -coordinate system for the Itakura-Saito Bregman manifold.

function of the Euclidean metric tensor g_{Euc} , the Itakura-Saito Bregman geometry is not conformal (see Figure 5).

Now, fix two points p and q , and let us seek for the third point r of the ∇ -triangle $\gamma_{pq}\gamma_{qr}\gamma_{rp}$ such that it holds both *simultaneously* that (i) $\gamma_{qr} \perp_q \gamma_{qp}$ (i.e., $\dot{\gamma}_{qr}(0) \perp_q \dot{\gamma}_{qp}(0)$) and (ii) $\gamma_{pq} \perp_p \gamma_{pr}$ (i.e., $\dot{\gamma}_{pq}(0) \perp_p \dot{\gamma}_{pr}(0)$). We end up with the following system of equations:

$$\begin{cases} \theta_r^\top \nabla^2 F(\theta_q) \theta_{pq} &= \theta_q^\top \nabla^2 F(\theta_q) \theta_{pq}, \\ \theta_r^\top \nabla^2 F(\theta_p) \theta_{pq} &= \theta_p^\top \nabla^2 F(\theta_p) \theta_{pq}. \end{cases} \quad (121)$$

It is a linear system $A\theta = b$ with

$$A = [a_{ij}] = \begin{bmatrix} \nabla^2 F(\theta_q) \theta_{pq} \\ \nabla^2 F(\theta_p) \theta_{pq} \end{bmatrix}, \quad b = [b_i] = \begin{bmatrix} \theta_q^\top \nabla^2 F(\theta_q) \theta_{pq} \\ \theta_p^\top \nabla^2 F(\theta_p) \theta_{pq} \end{bmatrix}. \quad (122)$$

When $\nabla^2 F(\theta) = Q \succ 0$ for a fixed positive-definite matrix and $p \neq q$, the system does not admit any solution (i.e., case of squared Mahalanobis distances which generalize the squared Euclidean distance and can have at most one right angle).

Otherwise, this linear system solves *uniquely* for asymmetric Bregman divergences [6] using Cramer's rule as

$$\theta_r^1 = \frac{\begin{vmatrix} b_1 & a_{12} \\ b_2 & a_{22} \end{vmatrix}}{|A|}, \quad \theta_r^2 = \frac{\begin{vmatrix} a_{11} & b_1 \\ a_{21} & b_2 \end{vmatrix}}{|A|}, \quad (123)$$

where $|\cdot|$ denotes the matrix determinant.

Similarly, we can build ∇^* -triangles with two right angles by exchanging $F \Leftrightarrow F^*$. Notice that having two right angles in a non-degenerate triangle makes it necessarily having an angle excess.

Figure 19 displays the following two double right angle ∇ -triangles (up to machine numerical precision) obtained for the following settings:

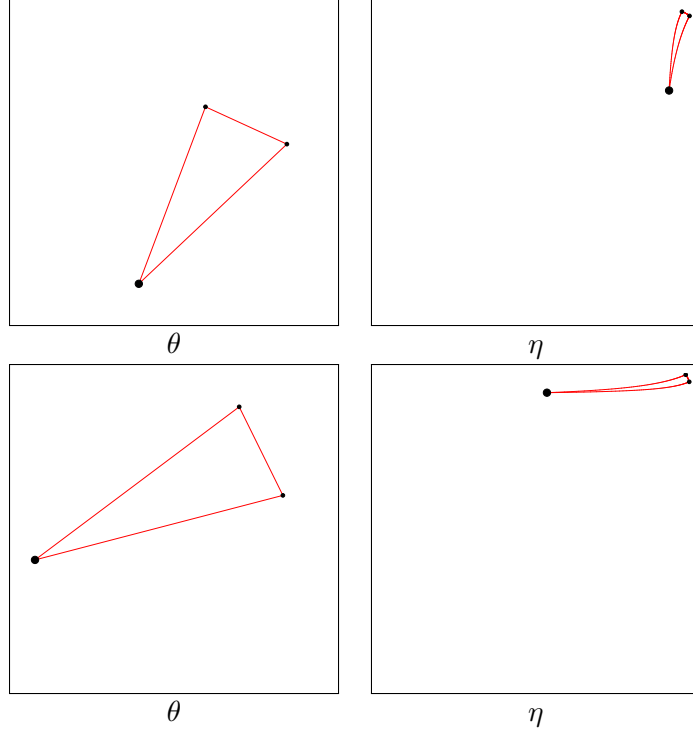


Figure 19: Two examples of ∇ -triangles with two interior right angles (the opposite angles to the thicker vertex r).

- $\theta(p) = (1.7372662352145616, 1.148396070619242)$,
 $\theta(q) = (1.241571556333764, 1.3768479188317202)$,
 $\theta(r) = (1.614143828700357, 1.8451358255393877)$,
 $\alpha_p(q, r) = 90.00000000000001$,
 $\alpha_q(p, r) = 90.0$,
 $\alpha_r(p, q) = 12.82764159141668$.
- $\theta(p) = (1.7128340504770114, 1.2510418358297621)$,
 $\theta(q) = (1.446857135939727, 1.7930125176801988)$,
 $\theta(r) = (1.1177842396781703, 1.5922051785236535)$,
 $\alpha_p(q, r) = 90.00000000000001$,
 $\alpha_q(p, r) = 90.00000000000001$,
 $\alpha_r(p, q) = 6.595093466701274$.

Define the following two θ -flat submanifolds:

$$H_q^\theta : \theta_r^\top \nabla^2 F(\theta_q) \theta_{pq} - \theta_q^\top \nabla^2 F(\theta_q) \theta_{pq} = 0, \quad (124)$$

$$H_p^\theta : \theta_r^\top \nabla^2 F(\theta_p) \theta_{pq} - \theta_p^\top \nabla^2 F(\theta_p) \theta_{pq} = 0. \quad (125)$$

We end up with the following proposition:

Proposition 2 *In a non-Mahalanobis Bregman manifold M , the locii of points r that form a double right angle with the geodesic arc γ_{pq} is $H_q^\theta \cap H_p^\theta$.*

Remember that the intersection of θ -flats is a θ -flat.

Notice that if instead of constraining two interior angles of a ∇ -triangle to have right angles, we ask for two *prescribed angles* $\alpha_q(p, r)$ and $\alpha_p(q, r)$, we would end up with the following system of non-linear equations to solve:

$$\begin{cases} \theta_{rq}^\top \nabla^2 F(\theta_q) \theta_{pq} &= \|\theta_{rq}\|_{\nabla^2 F(\theta_q)} \|\theta_{pq}\|_{\nabla^2 F(\theta_q)} \cos \alpha_q(p, r), \\ \theta_{rq}^\top \nabla^2 F(\theta_p) \theta_{pq} &= \|\theta_{rq}\|_{\nabla^2 F(\theta_p)} \|\theta_{pq}\|_{\nabla^2 F(\theta_p)} \cos \alpha_p(q, r). \end{cases} \quad (126)$$

Solving this non-linear system for r gives a solution whenever the system is feasible.

3.3 Geodesic ∇ -triangles with three interior right angles

Given a triple of points (p, q, r) , we may consider two fundamental types of triangles (up to duality and point permutations): a ∇ -triangle (type ppp) or a triangle of type pdp .

Let us consider a geodesic ∇ -triangle $\gamma_{pq}\gamma_{qr}\gamma_{rp}$ so that it holds simultaneously:

$$\gamma_{pq} \perp_p \gamma_{pr}, \quad \gamma_{qr} \perp_q \gamma_{qp}, \quad \gamma_{rp} \perp_r \gamma_{rq}. \quad (127)$$

Writing the above constraints in the primal θ -coordinate system, we end up with the following system to solve:

$$\begin{cases} \theta_{qp}^\top \nabla^2 F(\theta_p) \theta_{rp} &= 0 \\ \theta_{rq}^\top \nabla^2 F(\theta_q) \theta_{pq} &= 0 \\ \theta_{pr}^\top \nabla^2 F(\theta_r) \theta_{qr} &= 0. \end{cases} \quad (128)$$

Because of the Hessian matrices, this yields in general a non-linear system of equations to solve. The set of feasible solutions define the ∇ -triangles with three right angles. In dimension D , we have 3D unknown (the D θ -coordinates of the points p , q , and r) for 3 constraints. That is, the system is underconstrained.

For the 2D Itakura-Saito manifold, the Hessian matrix at p is $\text{diag}\left(\frac{1}{\text{sqr}(\theta_x)}, \frac{1}{\text{sqr}(\theta_y)}\right)$. Thus we get the following system to solve:

$$(\theta_q^x - \theta_p^x) \frac{1}{\text{sqr}(\theta_p^x)} (\theta_r^x - \theta_p^x) + (\theta_q^y - \theta_p^y) \frac{1}{\text{sqr}(\theta_p^y)} (\theta_r^y - \theta_p^y) = 0, \quad (129)$$

$$(\theta_r^x - \theta_q^x) \frac{1}{\text{sqr}(\theta_q^x)} (\theta_p^x - \theta_q^x) + (\theta_r^y - \theta_q^y) \frac{1}{\text{sqr}(\theta_q^y)} (\theta_p^y - \theta_q^y) = 0, \quad (130)$$

$$(\theta_p^x - \theta_r^x) \frac{1}{\text{sqr}(\theta_r^x)} (\theta_q^x - \theta_r^x) + (\theta_p^y - \theta_r^y) \frac{1}{\text{sqr}(\theta_r^y)} (\theta_q^y - \theta_r^y) = 0. \quad (131)$$

$$(132)$$

Multiplying Eq. 129 by $\text{sqr}(\theta_p^x)\text{sqr}(\theta_p^y)$, Eq. 130 by $\text{sqr}(\theta_q^x)\text{sqr}(\theta_q^y)$, and Eq. 131 by $\text{sqr}(\theta_r^x)\text{sqr}(\theta_r^y)$, we get a system of polynomial equations to solve [35]:

$$(\theta_q^x - \theta_p^x) \text{sqr}(\theta_p^y) (\theta_r^x - \theta_p^x) + (\theta_q^y - \theta_p^y) \text{sqr}(\theta_p^x) (\theta_r^y - \theta_p^y) = 0, \quad (133)$$

$$(\theta_r^x - \theta_q^x) \text{sqr}(\theta_q^y) (\theta_p^x - \theta_q^x) + (\theta_r^y - \theta_q^y) \text{sqr}(\theta_q^x) (\theta_p^y - \theta_q^y) = 0, \quad (134)$$

$$(\theta_p^x - \theta_r^x) \text{sqr}(\theta_r^y) (\theta_q^x - \theta_r^x) + (\theta_p^y - \theta_r^y) \text{sqr}(\theta_r^x) (\theta_q^y - \theta_r^y) = 0, \quad (135)$$

where $\text{sqr}(x) = x^2$. The system of polynomial equations has 3 equations with 6 positive variables defining 3 pairs of distinct points (θ_p^x, θ_p^y) , (θ_q^x, θ_q^y) , and (θ_r^x, θ_r^y) .

When considering the extended Kullback-Leibler manifold, since the Hessian matrix at p is $\text{diag}\left(\frac{1}{\theta_p^x}, \frac{1}{\theta_p^y}\right)$, we get the following system of polynomial equations (after multiplying the first equation by $\theta_p^x \theta_p^y$, the second equation by $\theta_q^x \theta_q^y$ and the third equation by $\theta_r^x \theta_r^y$):

$$\begin{cases} (\theta_q^x - \theta_p^x) \theta_p^y (\theta_r^x - \theta_p^x) + (\theta_q^y - \theta_p^y) \theta_p^x (\theta_r^y - \theta_p^y) = 0, \\ (\theta_r^x - \theta_q^x) \theta_q^y (\theta_p^x - \theta_q^x) + (\theta_r^y - \theta_q^y) \theta_q^x (\theta_p^y - \theta_q^y) = 0, \\ (\theta_p^x - \theta_r^x) \theta_r^y (\theta_q^x - \theta_r^x) + (\theta_p^y - \theta_r^y) \theta_r^x (\theta_q^y - \theta_r^y) = 0. \end{cases} \quad (136)$$

Fixing three variables, we get a cubic system of three equations in three unknowns. We used Wolfram alpha™ to check for potential real solution(s) of the system:

$$\begin{aligned} & a > 0, \quad b > 0, \quad c > a, \quad x > 0, \quad y > c, \quad z > 0, \\ & (c-a) * b * (y-a) + (x-b) * a * (z-b) = 0, \\ & (y-c) * x * (a-c) + (z-x) * c * (b-x) = 0, \\ & (a-y) * z * (c-y) + (b-z) * y * (x-z) = 0 \end{aligned}$$

The system does not admit solution in the positive orthant. We also checked the feasibility of the system for the Itakura-Saito manifold:

$$\begin{aligned} & a > 0, \quad b > 0, \quad c > a, \quad x > 0, \quad y > c, \quad z > 0, \\ & (c-a) * b * b * (y-a) + (x-b) * a * a * (z-b) = 0, \\ & (y-c) * x * x * (a-c) + (z-x) * c * c * (b-x) = 0, \\ & (a-y) * z * z * (c-y) + (b-z) * y * y * (x-z) = 0. \end{aligned}$$

The system does not admit solution in the positive orthant.

Thus it is an ongoing task to report an example of such a ∇ -triangle with three right angles for an asymmetric Bregman divergence, or to prove that such a triangle can never exist.

4 Simultaneous satisfying the dual Pythagorean theorems

Fix two points p and q of the Bregman manifold M . We seek for the locii of the third point $r \in M$ such that we have both $\gamma_{pq} \perp_q \gamma_{qr}^*$ and $\gamma_{pq}^* \perp_q \gamma_{qr}$. That is, we need to solve the following system of equations:

$$\begin{cases} (\eta(p) - \eta(q))^\top (\theta(r) - \theta(q)) = 0, \\ (\eta(p) - \eta(q))^\top (\theta(r) - \theta(q)) = 0. \end{cases} \quad (137)$$

Notice that finding such triples of points allow one to construct dual geodesic right-angle triangles. When $F(\theta) = \frac{1}{2} \theta^\top Q \theta$ for $Q \succ 0$ a positive-definite matrix, we have B_F that is a squared Mahalanobis distances, and the primal and dual geodesics coincide. Therefore any right-angle triangle is a dually right-angle solution to the problem in Mahalanobis manifolds. Thus we shall consider *asymmetric* Bregman divergences in the remainder since the only symmetric Bregman divergences are squared Mahalanobis distances [6].

4.1 Simultaneous dual orthogonality: A geometric interpretation

The constraint $\gamma_{pq} \perp_q \gamma_{qr}^*$ is equivalent to $(\theta(p) - \theta(q))^\top (\eta(r) - \eta(q)) = 0$. Let $\theta_{pq} = \theta(p) - \theta(q)$, $\eta_r = \eta(r)$ and $\eta_q = \eta(q)$. Then we have the following affine equation in η_r :

$$H^\eta(p, q) : \theta_{pq}^\top \eta_r - \theta_{pq}^\top \eta_q = 0. \quad (138)$$

The loci r of points satisfying the above equation is a $(D - 1)$ -dimensional ∇^* -autoparallel submanifold $H^\eta(p, q)$ (i.e., a $(D - 1)$ -dimensional η -flat [3] or loosely speaking a “ ∇^* -hyperplane”).

Similarly, the constraint $\gamma_{pq}^* \perp_q \gamma_{qr}$ is equivalent to $(\eta(p) - \eta(q))^\top (\theta(r) - \theta(q)) = 0$. Let $\eta_{pq} = \eta(p) - \eta(q)$, $\theta_r = \theta(r)$ and $\theta_q = \theta(q)$. Then we have the following affine equation in θ_r :

$$H^\theta(p, q) : \eta_{pq}^\top \theta_r - \eta_{pq}^\top \theta_q = 0. \quad (139)$$

The loci r of points satisfying the above equation is a $(D - 1)$ -dimensional ∇ -autoparallel submanifold $H^\theta(p, q)$ (i.e., a $(D - 1)$ -dimensional θ -flat [3] or ∇ -hyperplane).

Notice that point q ought to belong to both $H^\eta(p, q)$ and $H^\theta(p, q)$. Thus to simultaneously satisfy the two dual geodesic orthogonality constraints, the point r should belong to the intersection of a η -flat with a θ -flat:

$$S(p, q) = H^\eta(p, q) \cap H^\theta(p, q). \quad (140)$$

We should make sure $S(p, q)$ belongs to the manifold M when solving the equations using either the θ - or η -coordinate system.

Proposition 3 *The loci of points r such that $\gamma_{pq} \perp_q \gamma_{qr}^*$ and $\gamma_{pq}^* \perp_q \gamma_{qr}$ is the intersection of a θ -flat with a η -flat restricted to the manifold: $S(p, q) = H^\eta(p, q) \cap H^\theta(p, q)$.*

In general the intersection of a θ -flat with a η -flat is neither a θ -flat nor a η -flat. In 2D, the submanifolds $H^\eta(p, q)$ and $H^\theta(p, q)$ can be interpreted as a dual geodesic and a primal geodesic, respectively. Thus in 2D, S_{pq} may not be simply connected, and the maximum number of points of the intersection of two geodesics upper bounds the number of solutions for r . The next section illustrates how to build such triples of points for the Itakura-Saito manifold.

4.2 Explicit construction in the Itakura-Saito manifold

Consider the Itakura-Saito manifold described in §2.4.3. Let us exhibit some triple of points (p, q, r) such that $\gamma_{pq} \perp_q \gamma_{qr}^*$ and $\gamma_{pq}^* \perp_q \gamma_{qr}$. To avoid confusion, let us write the 2D θ - and η -coordinates of p by θ_p^x and θ_p^y , and η_p^x and η_p^y .

The second orthogonality constraint equation yields the equation $\eta_{pq}^\top (\theta_r - \theta_q) = \eta_{pq}^x \theta_r^x + \eta_{pq}^y \theta_r^y - \eta_{pq}^\top \theta_q = 0$ which can be rewritten as:

$$\theta_r^y = -\frac{\eta_{pq}^x}{\eta_{pq}^y} \theta_r^x + \frac{\eta_{pq}^\top \theta_q}{\eta_{pq}^y} = a \theta_r^x + b, \quad (141)$$

with $a = -\frac{\eta_{pq}^x}{\eta_{pq}^y}$ and $b = \frac{\eta_{pq}^\top \theta_q}{\eta_{pq}^y}$.

The first orthogonality constraint equation yields $(\theta_{pq})^\top (\eta_r - \eta_q)$ with $\eta_r^x = -\frac{1}{\theta_r^x}$ and $\eta_r^y = -\frac{1}{\theta_r^y}$. After multiplying both sides of the equation by $\theta_r^x \theta_r^y$, we find

$$-\theta_{pq}^x \theta_r^y - \theta_{pq}^y \theta_r^x - \theta_{pq}^\top \eta_q \theta_r^x \theta_r^y = 0 \quad (142)$$

Letting $\theta_r^y = a \theta_r^x + b$, we get the following quadratic equation to solve:

$$-\theta_{pq}^x (a \theta_r^x + b) - \theta_{pq}^y \theta_r^x - \theta_{pq}^\top \eta_q \theta_r^x (a \theta_r^x + b) = 0. \quad (143)$$

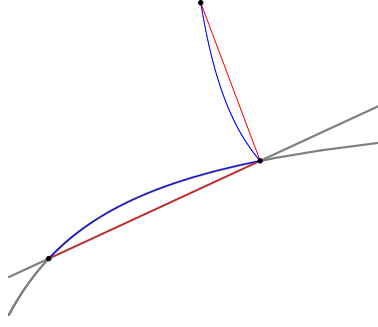


Figure 20: The intersection of $H^n(p, q)$ and $H^\theta(p, q)$ (displayed in black) yields two points: point q and the solution point r .

We write the former equation into the following canonical form of quadratic equations:

$$\underbrace{(-\theta_{pq}^\top \eta_q a)}_A (\theta_r^x)^2 + \underbrace{(-\theta_{pq}^x a - \theta_{pq}^y - b \theta_{pq}^\top \eta_q)}_B \theta_r^x + \underbrace{(-\theta_{pq}^x b)}_C = 0. \quad (144)$$

Then we solve the quadratic equation, and get the two solutions: Let $\Delta = B^2 - 4AC > 0$ be the discriminant. We have the two quadratic roots: $\theta_r^x = \frac{-B - \sqrt{\Delta}}{2A}$ and $\theta_r^x = \frac{-B + \sqrt{\Delta}}{2A}$, and we recover $\theta_r^{y'} = a\theta_r^{x'} + b$ and $\theta_r^{y''} = a\theta_r^{x''} + b$. One of the two solutions r' or r'' coincide with point q (with coordinate $\theta(q)$), so the solution point r is the remaining distinct point.

Figure 20 displays an example of a triple (p, q, r) with doubly right-angle at q with the pair of constraints $H^n(p, q)$ and $H^\theta(p, q)$ passing through point q .

Let us give a numerical example. Set

$$\theta(p) = (\theta_p^x, \theta_p^y) = (0.7273955397832663, 0.3279475469672596),$$

$$\theta(q) = (\theta_q^x, \theta_q^y) = (0.46251884248040354, 0.3902872167636309). \text{ Then we solve the quadratic equation and find the two solutions}$$

$$\theta(r) = (0.3065847355580658, 0.13822426240588664)$$

and

$$\theta(r'') = (0.4625188424804033, 0.39028721676363043).$$

Observe that $r'' = q$ so that the solution is $r = r'$. The triple (p, q, r') holds simultaneously the dual Pythagorean theorems at point q .

Figure 21 displays three examples of triples of points for which the dual Pythagorean theorems hold simultaneously. The triples of points displayed in Figure 21 are from left to right:

1. $\theta(p) = (0.9704854205553236, 1.4760141668100146)$,
 $\theta(q) = (1.141690604206171, 0.43035569351200803)$ and
 $\theta(r) = (0.22647618241885010, 0.34444830042268043)$.
2. $\theta(p) = (1.3163859900481611, 1.965380252548788)$,
 $\theta(q) = (1.5136826962585432, 1.2440688670072433)$ and
 $\theta(r) = (0.6359397574807304, 0.9494657726625966)$.

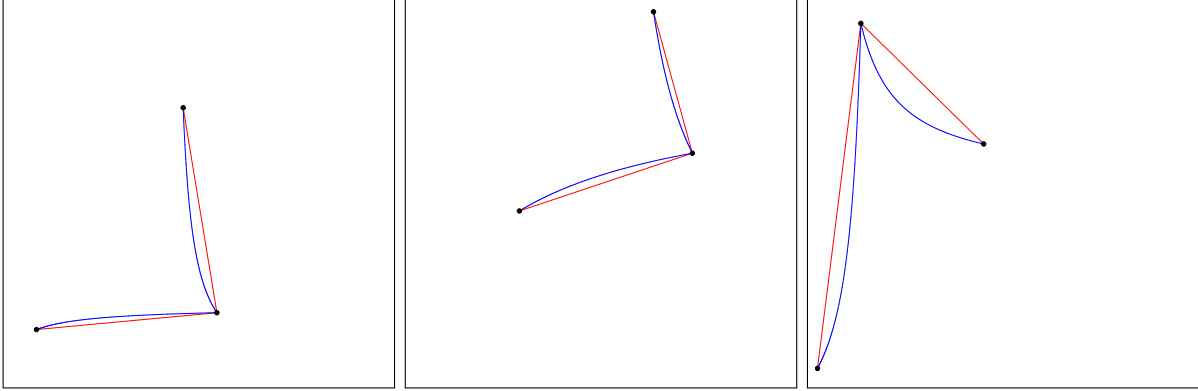


Figure 21: Three examples of triples of points (p, q, r) visualized in the θ -coordinate system for which the dual Pythagorean theorems hold simultaneously at q for the Burg negentropy generator. That is, we have both $\gamma_{pq} \perp_q \gamma_{qr}^*$ and $\gamma_{pq}^* \perp_q \gamma_{qr}$: The two pairs of (red,blue) geodesics form a right-angle at q : A “doubly right-angle”.

3. $\theta(p) = (0.9511702030611633, 1.291145089053253)$,
 $\theta(q) = (0.3277859642409383, 1.906447912395776)$ and
 $\theta(r) = (0.1077217190919158, 0.14622448026891943)$.

From these two pairs of dual right angle geodesic arcs at q , we can obtain four geodesic triangles by choosing either the primal or dual geodesic edge for the triangle edge pq : Namely, $\gamma_{pq}\gamma_{qr}\gamma_{rp}^*$, $\gamma_{pq}^*\gamma_{qr}\gamma_{rp}$ and $\gamma_{pq}\gamma_{qr}^*\gamma_{rp}$, $\gamma_{pq}^*\gamma_{qr}^*\gamma_{rp}$. These four triangles can be grouped into two dual pairs of dual geodesic triangles which exhibit a *dually right angle* at vertex q : $(\gamma_{pq}\gamma_{qr}\gamma_{rp}^*, \gamma_{pq}^*\gamma_{qr}^*\gamma_{rp})$ and $(\gamma_{pq}^*\gamma_{qr}\gamma_{rp}^*, \gamma_{pq}\gamma_{qr}^*\gamma_{rp})$.

Similarly, solving the dual orthogonality constraint at q for the cubic generator $F(\theta) = \frac{1}{3} \sum_i \theta_i^3$ yields a quadratic equation to solve. However, when considering the extended Shannon negentropy generator $F(\theta) = \sum_{i=1}^D \theta^i \log \theta^i - \theta^i$, we get a nonlinear equation (with sum of logarithmic terms) to solve: In 1D, we can easily run numerical optimization to approximate a solution numerically.

5 Conclusion

In a dually flat space [3] that we called a Bregman manifold in §2, geodesic triangles can either have angle excesses or angle defects like in arbitrary Riemannian geometry when the manifold is non self-dual (i.e., not of type Mahalanobis). First, we explained in §3 how to build geodesic ∇ -triangles with one, two or three right angles provided that the corresponding system of equations is feasible. The system of equations is linear up to two right angles but non-linear when dealing with three right angles. Second, we showed how to build triple of points (p, q, r) such that the dual Pythagorean theorems hold simultaneously at point q yielding a dually right angle at q : two dual pairs of right-angle dual geodesics. It turned out that the locii of such points r for given points p and q is the intersection of a η -flat with a θ -flat. We reported the explicit construction of such triples for the Itakura-Saito manifold in §4.2.

In future work, we shall consider dually flat spaces for symmetric positive-definite matrices [30, 22, 2] where the inner product is the trace of a matrix product. We would also like to prove the

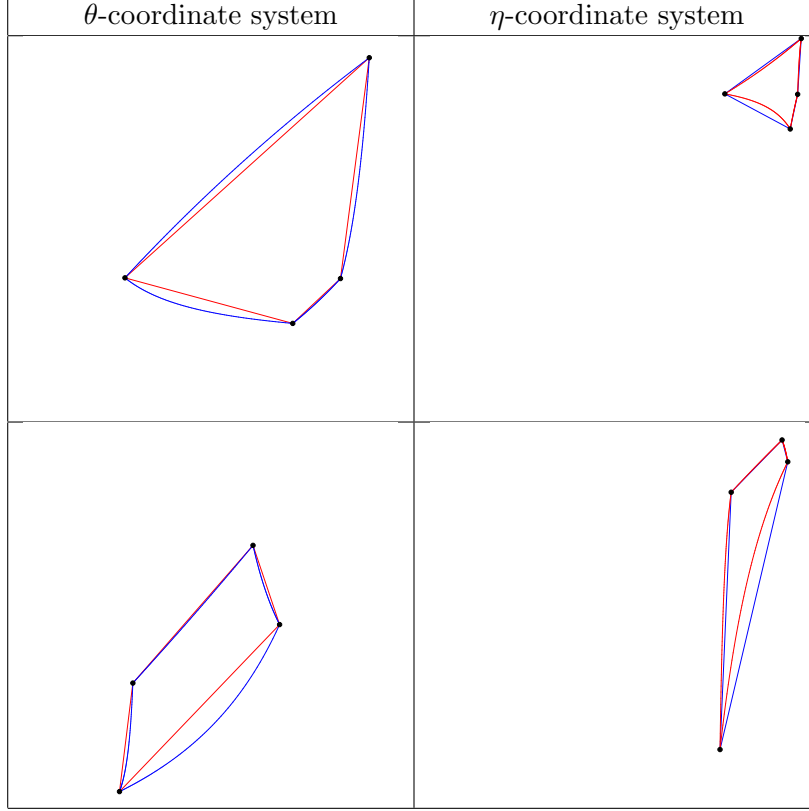


Figure 22: Examples of convex quadrangles in the Itakura-Saito manifold.

following experimental observation: For the 2D Burg negentropy generator, the total sum $\alpha(T)$ of the interior angles of a geodesic ∇ -triangle (geodesic triangle with all primal edges) plus the total sum $\beta = \alpha(T^*)$ of the interior angles of a dual geodesic ∇^* -triangle (geodesic triangle with all dual geodesic edges) sum up to 2π . For example, for $\theta(p) = (0.5, 0.5)$, $\theta(q) = (0.75, 0.75)$ and $\theta(r) = (0.95, 0.25)$, we find that $\alpha(T) = 160.19318300825412^\circ$ (angle defect), $\beta = \alpha(T^*) = 199.80681699174588^\circ$ (angle excess), and $\alpha + \beta = 360.0^\circ$. This property seems only to hold for the 2D Itakura-Saito divergence and not in higher dimensions.

We shall also consider an extension of this work to study properties of geodesic convex k -gons instead of geodesic triangles (i.e., 3-gons) in dually flat spaces (2^k such geodesic k -gons). For example, the Lambert quadrilaterals [32] (i.e., 4-gons) have three right angles and the remaining angle which is acute in hyperbolic geometry, obtuse in spherical geometry, and a right angle in Euclidean geometry. In a dually flat space, we have $2^4 = 16$ types of quadrilaterals defining overall $4 \times 4 = 16$ interior angles.⁹ Figure 22 displays all pairs of dual geodesics of some convex quadrilaterals in the θ - and η -coordinate systems.

Acknowledgments: Figures were programmed using `processing.org`

⁹A each quadrilateral vertex, we have 4 geodesics defining 6 interior angles between them.

References

- [1] Shotaro Akaho, Hideitsu Hino, and Noboru Murata. On a convergence property of a geometrical algorithm for statistical manifolds. *arXiv:1909.12644*, 2019.
- [2] Shun-ichi Amari. Information geometry of positive measures and positive-definite matrices: Decomposable dually flat structure. *Entropy*, 16(4):2131–2145, 2014.
- [3] Shun-ichi Amari. *Information geometry and its applications*, volume 194. Springer, 2016.
- [4] Katy S Azoury and Manfred K Warmuth. Relative loss bounds for on-line density estimation with the exponential family of distributions. *Machine Learning*, 43(3):211–246, 2001.
- [5] Arindam Banerjee, Srujana Merugu, Inderjit S Dhillon, and Joydeep Ghosh. Clustering with Bregman divergences. *Journal of machine learning research*, 6(Oct):1705–1749, 2005.
- [6] Jean-Daniel Boissonnat, Frank Nielsen, and Richard Nock. Bregman Voronoi diagrams. *Discrete & Computational Geometry*, 44(2):281–307, 2010.
- [7] Lev M. Bregman. The relaxation method of finding the common point of convex sets and its application to the solution of problems in convex programming. *USSR computational mathematics and mathematical physics*, 7(3):200–217, 1967.
- [8] Robert M Corless, Gaston H Gonnet, David EG Hare, David J Jeffrey, and Donald E Knuth. On the Lambert W function. *Advances in Computational mathematics*, 5(1):329–359, 1996.
- [9] Jean-Pierre Crouzeix. A relationship between the second derivatives of a convex function and of its conjugate. *Mathematical Programming*, 13(1):364–365, 1977.
- [10] Imre Csiszár. Information-type measures of difference of probability distributions and indirect observation. *studia scientiarum Mathematicarum Hungarica*, 2:229–318, 1967.
- [11] Stephen Della Pietra, Vincent Della Pietra, and John Lafferty. Inducing features of random fields. *IEEE transactions on pattern analysis and machine intelligence*, 19(4):380–393, 1997.
- [12] Herbert Edelsbrunner and Hubert Wagner. Topological data analysis with Bregman divergences. In *33rd International Symposium on Computational Geometry (SoCG 2017)*. Schloss Dagstuhl-Leibniz-Zentrum fuer Informatik, 2017.
- [13] Shinto Eguchi et al. Geometry of minimum contrast. *Hiroshima Mathematical Journal*, 22(3):631–647, 1992.
- [14] Luther Pfahler Eisenhart. *Riemannian geometry*. Princeton university press, 1997.
- [15] Takashi Kurose. Dual connections and affine geometry. *Mathematische Zeitschrift*, 203(1):115–121, 1990.
- [16] Stefan L. Lauritzen. Statistical manifolds. *Differential geometry in statistical inference*, 10:163–216, 1987.
- [17] Prasanta Chandra Mahalanobis. On the generalized distance in statistics. *Proceedings of the National Institute of Sciences (Calcutta)*, 2:49–55, 1936.

- [18] Frank Nielsen. Legendre transformation and information geometry, 2010.
- [19] Frank Nielsen. Cramér-Rao lower bound and information geometry. In *Connected at Infinity II*, pages 18–37. Springer, 2013.
- [20] Frank Nielsen. An elementary introduction to information geometry. *arXiv:1808.08271*, 2018.
- [21] Frank Nielsen. On geodesic triangles with right angles in a dually flat space. *Progress in Information Geometry: Theory and Applications*, pages 153–190, 2021.
- [22] Frank Nielsen and Rajendra Bhatia. *Matrix information geometry*. Springer, 2013.
- [23] Frank Nielsen and Sylvain Boltz. The Burbea-Rao and Bhattacharyya centroids. *IEEE Transactions on Information Theory*, 57(8):5455–5466, 2011.
- [24] Frank Nielsen and Vincent Garcia. Statistical exponential families: A digest with flash cards. *arXiv:0911.4863*, 2009.
- [25] Frank Nielsen and Gaëtan Haderes. Monte Carlo information geometry: The dually flat case. *arXiv preprint arXiv:1803.07225*, 2018.
- [26] Frank Nielsen, Boris Muzellec, and Richard Nock. Classification with mixtures of curved Mahalanobis metrics. In *2016 IEEE International Conference on Image Processing (ICIP)*, pages 241–245. IEEE, 2016.
- [27] Frank Nielsen and Richard Nock. Sided and symmetrized Bregman centroids. *IEEE transactions on Information Theory*, 55(6):2882–2904, 2009.
- [28] Frank Nielsen and Richard Nock. Skew Jensen-Bregman voronoi diagrams. In *Transactions on Computational Science XIV*, pages 102–128. Springer, 2011.
- [29] Frank Nielsen and Richard Nock. On the geometry of mixtures of prescribed distributions. In *IEEE International Conference on Acoustics, Speech and Signal Processing (ICASSP)*, pages 2861–2865. IEEE, 2018.
- [30] Richard Nock, Brice Magdalou, Eric Briys, and Frank Nielsen. Mining matrix data with Bregman matrix divergences for portfolio selection. In *Matrix Information Geometry*, pages 373–402. Springer, 2013.
- [31] Aleksandr Petrovich Norden. On pairs of conjugate parallel displacements in multidimensional spaces. *Dokl. Akad. Nauk SSSR*, 49(9):1345–1347, 1945.
- [32] Boris A. Rosenfeld. *A history of non-Euclidean geometry: Evolution of the concept of a geometric space*, volume 12. Springer Science & Business Media, 2012.
- [33] R. N. Sen. Parallel displacement and scalar product of vectors. In *Proceedings of the National Institute of Sciences of India*, volume 14, page 45. National Institute of Sciences of India, 1948.
- [34] Hirohiko Shima. *The geometry of Hessian structures*. World Scientific, 2007.
- [35] Bernd Sturmfels. *Solving systems of polynomial equations*. American Mathematical Soc., 2002. 97.

- [36] Joseph Albert Wolf. *Spaces of constant curvature*, volume 372. American Mathematical Soc., 1972.
- [37] Ting-Kam Leonard Wong. Logarithmic divergences from optimal transport and Rényi geometry. *Information Geometry*, 1(1):39–78, 2018.

A Notations

F	Strictly convex and C^3 real-valued function
F^*	Dual Legendre-Fenchel convex conjugate
$\theta(p) = (\theta^1(p), \dots, \theta^D(p))$	primal coordinates of point p
$\eta(p) = (\eta_1(p), \dots, \eta_D(p))$	dual coordinates of point p
$\theta_{ab} = \theta_a - \theta_b$	notational shortcut
$\eta_{ab} = \eta_a - \eta_b$	notational shortcut
$D_F(p : q)$	Divergence between points
$B_F(\theta(p) : \theta(q))$	Bregman divergence
$A_F(\theta(p) : \eta(q))$	Fenchel-Young divergence
(M, g, ∇, ∇^*)	Dually flat space (Bregman manifold)
T_p	Tangent plane at p
$g_p(u, v)$	inner product between two vectors u and v of T_p
$[g_{ij}] = [g(e_i, e_j)]_{ij} = \nabla^2 F(\theta)$	Riemannian metric
$[g^{*ij}] = [g^*(e^{*i}, e^{*j})]_{ij} = \nabla^2 F^*(\eta)$	dual Riemannian metric
$\prod_{p,q}(v)$	primal parallel transport of $v \in T_p$ to T_q
$\prod_{p,q}^*(v)$	dual parallel transport of $v \in T_p$ to T_q
$\gamma_{ab}(t)$	Primal geodesic: $\theta(\gamma_{ab}(t)) = (1-t)\theta(a) + t\theta(b)$
$\gamma_{ab}(t)^*$	Dual geodesic: $\eta(\gamma_{ab}^*(t)) = (1-t)\eta(a) + t\eta(b)$
$(v)_B$	vector components in basis B , arranged in a D -tuple
$[v]_B$	vector components in basis B , arranged in a D -dimensional column vector
$B_p = \{e_i = \partial_i = \frac{\partial}{\partial \theta^i}\}$	natural basis at T_p
$B_p^* = \{e^{*i} = \partial^i = \frac{\partial}{\partial \eta_i}\}_i$	reciprocal basis at T_p so that $g(e_i, e^{*j}) = \delta_i^j$
$v_{ab} = \frac{d}{dt} \gamma_{ab}(0) = \dot{\gamma}_{ab}(0)$	tangent vector of $\gamma_{ab}(t)$ at a with contravariant components $\theta(b) - \theta(a)$
$v_{ab}^* = \frac{d}{dt} \gamma_{ab}^*(0) = \dot{\gamma}_{ab}^*(0)$	tangent vector of $\gamma_{ab}^*(t)$ at a with covariant components $\eta(b) - \eta(a)$
$[v^i]_B$	contravariant components of vector v , $v^i = g(v, e^{*i})$
$[v_i]_B$	covariant components of vector v (meaning $[v]_{B^*}$), $v_i = g(v, e_i)$
$g_p(u, v)$	inner product at T_p of two vectors: $g_p(u, v) = u_i v^i = u^i v_i$